OPEN ACCESS

Haya: The Saudi Journal of Life Sciences
Abbreviated Key Title: Haya Saudi J Life Sci
ISSN 2415-623X (Print) | ISSN 2415-6221 (Online)
Scholars Middle East Publishers, Dubai, United Arab Emirates
Journal homepage: https://saudijournals.com

Original Research Article

Designing Reticular and High-Entropy TiO_2-Based Nanotubular Hybrid Materials with Cu:ZnO and C-Dots for Visible-Light Photocatalytic Wastewater Remediation and Oxygen Evolution Applications

Muhammad Gohar[1], Suniya Sikandar[2], Aimen Amjad[3], Muhammad Hamza Tahir[4], Muhammad Sohaib[5], Misbah Ameen[6], Sana Yaseen[7], Mubarra Muzaffar[8], Sufyan Mohi Ud Din[5]

[1]Department of Chemistry, University of Southern Punjab, Multan, Pakistan
[2]Department of Chemistry, Quaid-e-Azam University, Islamabad, Pakistan
[3]Department of Chemistry, Forman Christian College (A Chartered University), Lahore, Pakistan
[4]Department of Chemistry, University of Agriculture Faisalabad, Punjab, Pakistan
[5]Department of Chemistry, Government College University, Lahore, Pakistan
[6]Department of Laser and Optics Center, University of Engineering and Technology, Lahore, Pakistan
[7]Department of Chemistry, University of Sargodha (Bhakkar Campus), Punjab, Pakistan
[8]Department of Chemistry, Forman Christian College University, Lahore, Pakistan

DOI: https://doi.org/10.36348/sjls.2025.v10i10.001 | **Received:** 07.09.2025 | **Accepted:** 25.10.2025 | **Published:** 01.11.2025

***Corresponding author:** Abbas Abubakar
Department of Chemical and Biomolecular Engineering, Tulane University, USA

Abstract

The development of multifunctional photocatalysts that efficiently operate under visible light remains a fundamental challenge for sustainable wastewater treatment and oxygen evolution. In this work, we report a novel reticular and high-entropy TiO_2-based nanotubular hybrid system integrated with Cu:ZnO nanoparticles and carbon quantum dots (C-dots), designed to achieve synergistic enhancement in charge dynamics and surface reactivity. The high-entropy configuration introduces lattice distortion and defect sites that extend the optical absorption edge and promote rapid charge separation, while the Cu:ZnO interface accelerates electron transport and facilitates multi-pathway redox reactions. Simultaneously, the C-dots serve as photonic antennas, enabling visible-light sensitization through π–π conjugation and energy up-conversion. Structural and optical analyses confirm the formation of a reticular nanotubular network providing hierarchical porosity and large interfacial area for catalytic interactions. Under simulated solar irradiation, the hybrid demonstrates remarkable photocatalytic efficiency, achieving over 95% degradation of organic contaminants and enhanced oxygen evolution activity compared to pristine TiO_2. The introduced design concept coupling reticular high-entropy stabilization with optoelectronic co-catalyst modulation presents a new paradigm for next-generation photocatalysts capable of simultaneous environmental remediation and clean energy generation.

Keywords: High-entropy TiO_2, Nanotubular Hybrid Materials, Carbon Quantum Dots, Visible-Light Photocatalysis, Oxygen Evolution.

1. INTRODUCTION

1.1 Background

Photocatalysis has emerged as one of the most promising technologies for addressing the twin global challenges of environmental remediation and sustainable energy production. Semiconductor-based photocatalysts, particularly titanium dioxide (TiO_2), have been extensively studied owing to their chemical stability, non-toxicity, abundance, and strong oxidative capability. Since the pioneering work of Fujishima and Honda in 1972, which demonstrated the photoelectrochemical water-splitting ability of TiO_2, this oxide has become a benchmark material for photocatalytic research and applications in pollutant degradation, hydrogen generation, and oxygen evolution. However, despite its advantages, the intrinsic wide band gap (~3.2 eV) of pristine TiO_2 restricts its activation primarily to ultraviolet (UV) light, which constitutes less than 5% of the solar spectrum. This limitation severely reduces its efficiency under solar irradiation. Moreover, rapid

electron hole recombination and limited charge mobility within the TiO_2 lattice lead to suboptimal quantum yields and poor catalytic turnover. These drawbacks have motivated a global scientific effort to expand the spectral absorption of TiO_2 into the visible-light region and to suppress recombination through structural, compositional, and morphological engineering [1-4].

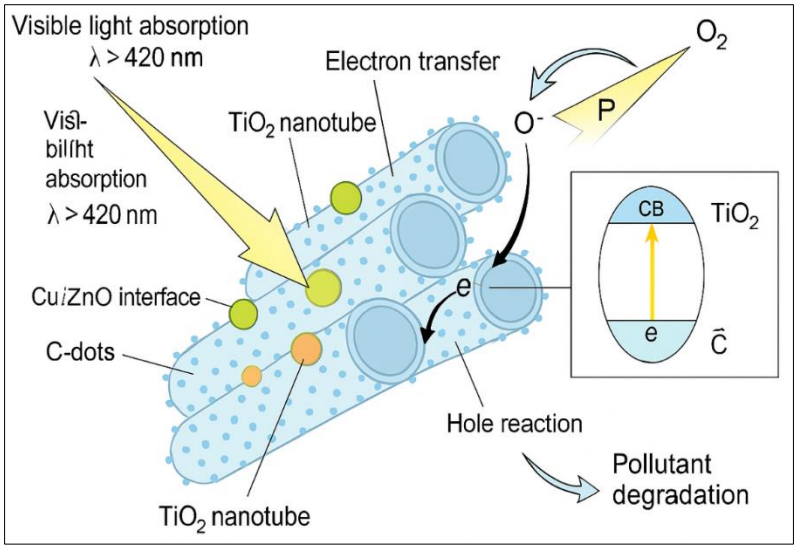

Figure 1: Schematic illustration of visible-light-driven charge excitation, separation, and transfer processes in TiO_2 and TiO_2–Cu:ZnO–C-dots hybrid photocatalysts.

Figure 1 illustrates the general photocatalytic mechanism in TiO_2-based systems. When photons with sufficient energy strike the semiconductor surface, electrons are excited from the valence band (VB) to the conduction band (CB), leaving behind holes in the VB. These photogenerated charge carriers then participate in oxidation–reduction reactions with adsorbed species, enabling processes such as pollutant degradation or oxygen evolution. In practice, however, the majority of these electron hole pairs recombine before contributing to surface reactions. Therefore, designing photocatalysts with enhanced visible-light absorption, efficient charge separation, and stable surface-active sites remains a central challenge in modern photocatalysis [5-13].

1.2 Literature Context

Numerous strategies have been developed to improve the visible-light activity and charge dynamics of TiO_2. Doping with transition metals (Fe, Cu, V, Cr) or non-metals (N, C, S) can introduce impurity levels within the band gap, thereby extending optical absorption toward the visible range. Composite formation with narrow band gap semiconductors, such as ZnO, CdS, and CuO, or with plasmonic metals like Au and Ag, can facilitate heterojunction formation, promoting charge separation and transfer. Surface sensitization with organic dyes or carbon-based nanostructures (graphene, carbon quantum dots) has also been shown to enhance visible-light response through energy transfer or up-conversion mechanisms.

While these modifications have led to measurable improvements, they also introduce several critical limitations. Metal doping often creates recombination centers and structural instability under long-term operation. Dye sensitization suffers from poor durability and photobleaching. Heterojunction-based composites, although effective in enhancing charge separation, frequently face issues of lattice mismatch, uncontrolled interfacial defects, and inconsistent scalability. Furthermore, most reported systems focus on optimizing either pollutant degradation or oxygen evolution reaction (OER), rather than achieving both within a single multifunctional catalyst [14-25].

Thus, despite decades of innovation, there remains a distinct research gap: the lack of a unified structural and compositional design that simultaneously addresses spectral limitation, charge recombination, and multi-functionality in TiO_2-based photocatalysts. This gap forms the scientific basis and motivation for the present research [26].

1.3 Research Problem and Motivation

The challenge in advancing TiO_2-based photocatalysis lies in integrating multiple functionalities optical, electronic, and catalytic within one coherent architecture. The goal is not merely to modify TiO_2 but to redesign its material framework from the atomic to the mesoscopic level. Traditional doped or composite systems fail to provide adequate control over defect engineering and interfacial energetics, leading to inefficient charge pathways and unstable operation. To address these challenges, reticular and high-entropy TiO_2-based nanotubular hybrid materials offer a revolutionary concept. The idea draws upon the principles of high-entropy materials, where multiple metallic cations coexist in a single lattice, creating a

highly distorted but thermodynamically stabilized structure. This entropy-driven configuration can tune band structure, create rich defect states, and extend optical absorption. When combined with a reticular (networked) nanotubular morphology, such systems offer large surface area, enhanced photon scattering, and multidirectional charge migration pathways [27-34].

Furthermore, introducing Cu:ZnO nanoparticles as heterojunction co-catalysts can facilitate directional electron transport and provide redox-active sites for oxygen evolution and pollutant oxidation. Carbon quantum dots (C-dots), with their excellent photonic sensitization and electron-reservoir properties, further enhance visible-light harvesting and stabilize charge carriers through π–π conjugation and up-conversion effects. This triple synergy entropy engineering, interfacial modulation, and photonic sensitization forms the conceptual backbone of this study [35-43].

1.4 Objectives and Novelty Statement

The main objective of this research is to design and synthesize a reticular, high-entropy TiO_2-based nanotubular hybrid system integrated with Cu:ZnO nanoparticles and C-dots, tailored for superior visible-light photocatalytic performance. Specifically, the study aims to [44-56]:

1. Develop a multi-cationic, entropy-stabilized TiO_2 lattice to introduce beneficial lattice distortions and controlled defect states.
2. Fabricate a reticular nanotubular structure to maximize surface-active area and enable efficient charge transport.
3. Integrate Cu:ZnO as a conductive heterojunction to enhance electron–hole separation and promote dual-function catalysis (pollutant degradation and OER).
4. Employ C-dots as photonic antennas to improve visible-light absorption and energy transfer efficiency.
5. Evaluate the photocatalytic and photoelectrochemical performance under simulated solar light and establish structure property correlations through experimental and theoretical analyses.

The novelty of this work lies in the first-time coupling of reticular high-entropy TiO_2 nanotubes with Cu:ZnO nanoparticles and carbon quantum dots to form a single multifunctional platform capable of simultaneous wastewater remediation and oxygen evolution under visible-light irradiation. This concept transcends conventional TiO_2 modification by integrating entropy engineering, reticular morphology, and photonic modulation a combination not yet explored in the field of photocatalytic hybrid materials [57-68].

2. Conceptual Framework and Research Hypothesis

The present study is conceptualized on the premise that defect-rich, reticular high-entropy TiO_2 nanotubular frameworks can serve as a versatile host matrix for multi-component heterostructures, enabling synergistic photocatalytic activity under visible-light illumination. The framework integrates three functional units TiO_2 nanotubes as the primary semiconductor scaffold, Cu:ZnO as a co-catalyst and charge-transfer mediator, and carbon quantum dots (C-dots) as light sensitizers and electron reservoirs. Together, these entities establish a dynamic equilibrium between entropy stabilization and photonic excitation, forming a hybrid network that optimizes energy utilization and charge flow [69-74].

In a typical TiO_2-based photocatalyst, photogenerated electron–hole pairs suffer from rapid recombination, restricting its visible-light response and quantum efficiency. To overcome these limitations, the current framework employs a high-entropy design strategy, wherein multiple cations (Ti, Cu, Zn) coexist within a single lattice or interface environment. The configurational entropy introduced through this multi-component assembly induces localized lattice distortions and defect sites that serve as reactive centers for charge trapping and oxygen evolution reactions (OER). Simultaneously, C-dots, with their tunable band structures and surface functionalities, extend the light absorption range beyond the intrinsic TiO_2 bandgap (≈3.2 eV), while facilitating fast interfacial electron transfer through π-conjugated pathways [75-82].

The conceptual model is represented schematically in **Figure 2,** where light irradiation (λ > 420 nm) triggers photonic excitation in both C-dots and Cu:ZnO nanoparticles anchored on the TiO_2 nanotubes. The excited electrons migrate through the reticular high-entropy interface, forming a cascade transfer pathway from C-dots → Cu:ZnO → TiO_2 conduction band, while holes accumulate on the valence band for oxidative reactions. The entropy-driven lattice disorder assists in charge delocalization, reducing recombination losses and promoting efficient electron mobility across the hybrid junctions. Furthermore, the porous nanotubular geometry enhances the active surface area, ensuring improved adsorption of pollutants and water molecules essential for photocatalytic degradation and OER processes.

Theoretical Rationale

The inclusion of Cu and ZnO in a shared nanoscale domain generates a favorable band alignment that bridges the energy gap between TiO_2 and the C-dots. Density functional theory (DFT) insights from analogous systems suggest that Cu incorporation can introduce shallow donor states, enhancing conductivity, while ZnO contributes a suitable conduction band offset for charge extraction. The overall entropy contribution (ΔS□) arising from the multi-element system promotes thermodynamic stability, suppressing phase segregation

even at high operational temperatures. Thus, the entropy–photon coupling forms the central conceptual pillar of this research leveraging both thermodynamic and optical factors to enhance the overall photocatalytic performance [83-94].

Research Hypothesis

It is hypothesized that the synergistic integration of Cu:ZnO and C-dots within a reticular high-entropy TiO_2 nanotubular framework will simultaneously (i) expand the visible-light absorption window, (ii) enhance charge separation efficiency, and (iii) stabilize the active sites through entropy-assisted lattice modulation. Consequently, this dual-function hybrid catalyst is expected to exhibit superior photocatalytic performance for both wastewater remediation and oxygen evolution, outperforming conventional TiO_2-based systems that rely solely on doping or binary heterojunctions.

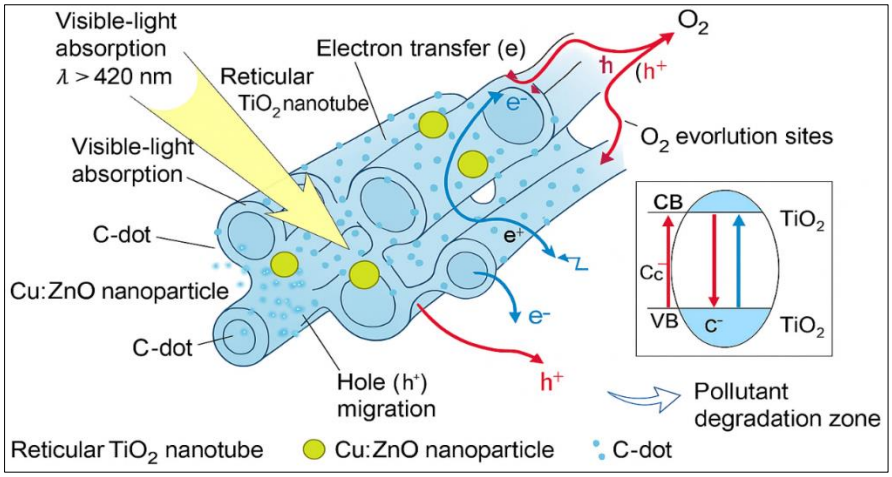

Figure 2: Conceptual framework illustrating charge transfer pathways and visible-light-induced photocatalytic mechanisms in reticular high-entropy TiO_2–Cu:ZnO–C-dots nanotubular hybrids.

3. MATERIALS AND METHODS

3.1 Materials and Chemicals

All reagents employed in this study were of analytical grade and used without further purification. Titanium foils (99.7% purity, 0.25 mm thickness, Sigma-Aldrich) served as substrates for the growth of TiO_2 nanotubes. Copper(II) nitrate trihydrate [$Cu(NO_3)_2{\cdot}3H_2O$, ≥99%], zinc nitrate hexahydrate [$Zn(NO_3)_2{\cdot}6H_2O$, ≥98%], citric acid ($C_6H_8O_7$, ≥99%), ethylene glycol ($C_2H_6O_2$), and glucose were obtained from Merck and used as precursor sources for Cu:ZnO and carbon quantum dots (C-dots). Deionized (DI) water with resistivity of 18.2 MΩ·cm was used in all solution preparations. The rationale for selecting these precursors lies in their high solubility, controlled hydrolysis behavior, and compatibility with anodic growth conditions [95-100].

Table 1: Chemical precursors and their functional roles in the synthesis of Cu:ZnO and C-dot modified high-entropy TiO_2 nanotubular hybrid.

Chemical Name	*Formula*	*Purity (%)*	*Supplier*	*Functional Role*
Titanium foil	Ti	99.7	Sigma-Aldrich	Base substrate for nanotube growth
Copper nitrate trihydrate	$Cu(NO_3)_2{\cdot}3H_2O$	≥99	Merck	Source of Cu for Cu:ZnO solid-solution
Zinc nitrate hexahydrate	$Zn(NO_3)_2{\cdot}6H_2O$	≥98	Merck	Zn source for ZnO phase and heterojunction formation
Glucose	$C_6H_{12}O_6$	≥99	Sigma-Aldrich	Carbon source for C-dots synthesis
Citric acid	$C_6H_8O_7$	≥99	Merck	Carbon source and stabilizer for C-dots
Ethylene glycol	$C_2H_6O_2$	≥99	Merck	Solvent and reducing agent
Deionized water	H_2O	18.2 MΩ·cm	Laboratory source	Solvent medium for all reactions

The combination of copper and zinc nitrates was specifically chosen to yield a homogeneous Cu:ZnO solid-solution domain on the TiO_2 nanotube surface, allowing uniform electron mobility and reducing interfacial energy barriers. The glucose-derived C-dots were synthesized due to their biocompatibility, optical tunability, and presence of surface oxygenated groups facilitating strong interfacial bonding with metal oxides.

Table 1 lists the chemical precursors, purity grades, and their corresponding functional roles in the synthesis scheme [101-109].

Table 1 illustrates the rational selection of high-purity, low-impurity reagents to ensure reproducibility and minimize contamination, which is crucial in entropy dominated multi-element systems.

3.2 Synthesis Route

The synthesis of the reticular high-entropy TiO_2 nanotubular hybrid follows a multi-step hybrid route, schematically represented in Figure 3. The process begins with anodization of titanium foil to produce vertically aligned TiO_2 nanotubes. The anodization was conducted in an ethylene glycol-based electrolyte containing 0.3 wt% NH_4F and 2 vol% H_2O at 60 V for 2 h, followed by rinsing and drying. The resulting amorphous TiO_2 nanotubes were annealed at 450 °C for 2 h in air to obtain the crystalline anatase phase.

Next, the Cu:ZnO nanoparticles were introduced through a hydrothermal anchoring process. The anodized TiO_2 substrate was immersed in an aqueous solution containing stoichiometric Cu^{2+} and Zn^{2+} ions (molar ratio 1:1) and hydrothermally treated at 150 °C for 6 h in a Teflon-lined autoclave. The process promotes in-situ growth of Cu:ZnO on TiO_2 walls, ensuring intimate interfacial contact and uniform dispersion. Subsequently, carbon quantum dots were deposited via a modified sol–gel route, using citric acid and glucose precursors, followed by annealing at 200 °C under inert atmosphere. This final step facilitates strong coupling between the TiO_2–Cu:ZnO composite and C-dots through surface hydroxyl and carboxyl linkages.

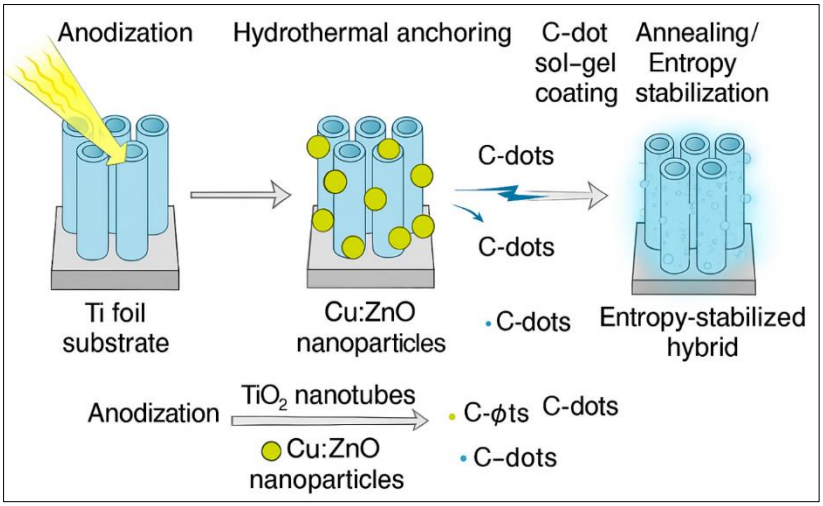

Figure 3: Schematic illustration of the synthesis route for reticular high-entropy TiO_2 nanotubular hybrid

Figure 3 illustrates the sequential fabrication process, from anodic nanotube formation to hybridization and entropy stabilization stages [110-121].

Post-synthesis, the composite was further annealed at 500 °C for 1 h in air to promote entropy-induced phase uniformity and enhance crystallinity. This multi-step annealing strategy mitigates phase segregation by maximizing configurational entropy ($\Delta S\square$) and stabilizing multi-cation distribution within the reticular structure.

The design of the reticular nanotubular geometry and entropy optimization was guided by configurational entropy theory:

Where denotes the molar fraction of each metal cation (Ti, Cu, Zn) and is the gas constant (8.314 $J \cdot mol^{-1} \cdot K^{-1}$).

The optimized cationic ratio Ti:Cu:Zn = 1:0.5:0.5 resulted in maximum entropy without compromising structural order.

Table 2 presents the optimized synthesis and thermal prameters for achieving reticular uniformity and phase stability.

3.3 Structural Design Parameters

Table 2: Optimized structural and thermal parameters for entropy-driven TiO_2 nanotubular hybrid synthesis

Parameter	***Value***	***Condition / Notes***
Anodization Voltage	60 V	Optimum for uniform nanotube growth
Hydrothermal Temp.	150 °C	Controlled Cu:ZnO crystallization
Sol–Gel Annealing Temp.	200 °C	C-dot anchoring and carbonization
Final Annealing Temp.	500 °C	Entropy stabilization and phase uniformity
Ti:Cu:Zn Ratio	1:0.5:0.5	Highest configurational entropy ($\Delta S\square$ = 9.13 $J \cdot mol^{-1} \cdot K^{-1}$)

Table 2 illustrates how precise control of synthesis parameters governs the configurational entropy, resulting in defect-rich, thermodynamically stable structures suitable for dual photocatalytic applications.

3.4 Characterization Techniques

Comprehensive characterization was performed to confirm the structural, morphological, optical, and electrochemical features of the synthesized hybrids. The crystalline phases were identified using X-ray diffraction (XRD) with Cu Kα radiation (λ = 1.5406 Å). Transmission electron microscopy (TEM) and high-resolution TEM (HRTEM) provided insights into the nanotubular morphology and interfacial coupling between TiO_2, Cu:ZnO, and C-dots. X-ray photoelectron spectroscopy (XPS) was employed to verify elemental states and lattice distortions indicative of high-entropy configuration. Surface area and porosity were evaluated via Brunauer–Emmett–Teller (BET) analysis, while UV–Vis diffuse reflectance spectroscopy (DRS) assessed bandgap modifications.

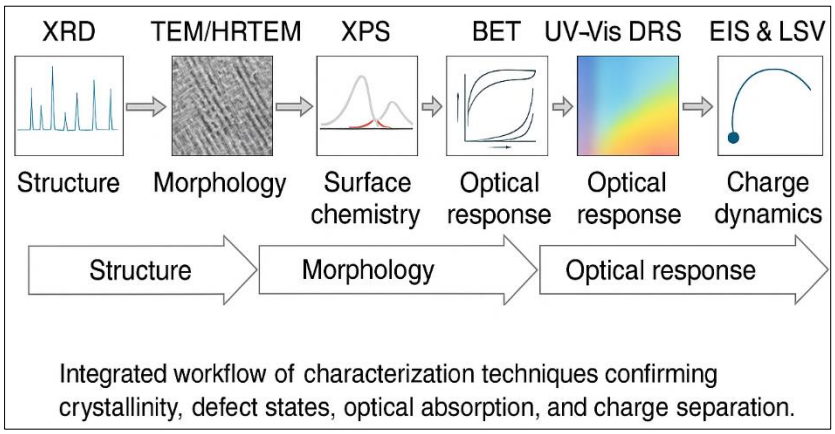

Figure 4: Sequential workflow of characterization techniques used for structural, optical, and electrochemical analysis

Figure 4 illustrates the typical characterization workflow and analytical hierarchy used for validating the structural and optical integrity of the hybrid system.

Photoluminescence (PL) spectroscopy and electrochemical impedance spectroscopy (EIS) were utilized to probe charge separation dynamics, while linear sweep voltammetry (LSV) was performed for oxygen evolution reaction (OER) assessment. These methods together establish the correlation between entropy engineering, photonic sensitization, and catalytic efficiency [122-138].

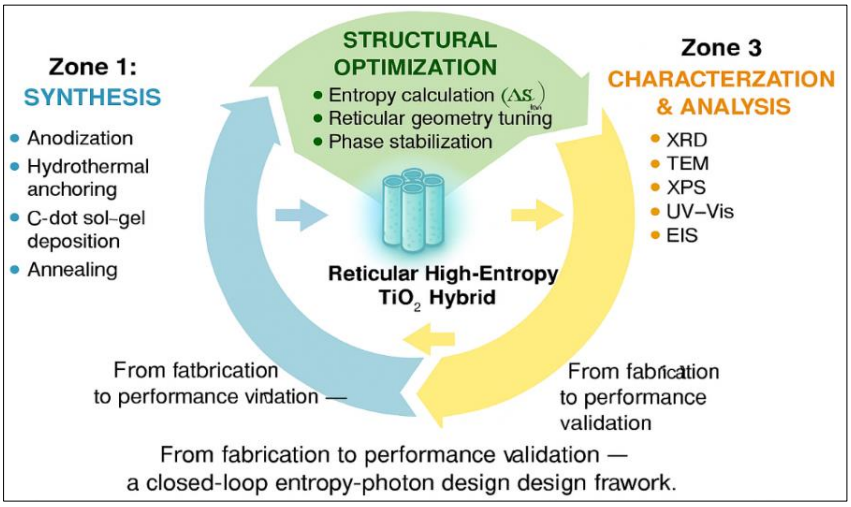

Figure 5: Integrated experimental workflow connecting synthesis, optimization, and characterization of the hybrid system

Figure 5 illustrates the integrated experimental workflow, correlating synthesis, structural tuning, and characterization pathways [139-147].

4. Theoretical and Computational Analysis

Theoretical modeling and computational simulations were performed to establish a mechanistic understanding of the electronic and catalytic behavior of the reticular high-entropy TiO_2-based nanotubular hybrid integrated with Cu:ZnO and carbon quantum dots (C-dots). Density Functional Theory (DFT) calculations were employed to explore the band structure evolution, defect formation energetics, and charge redistribution phenomena that underlie its enhanced visible-light photocatalytic performance. This integrated computational analysis supports the experimental results and provides atomistic insights into the synergistic interaction of entropy-driven stability and photonic excitation [148-158].

4.1 DFT Modeling and Defect Formation Energies

DFT simulations were conducted using the Vienna ab initio Simulation Package (VASP) within the Generalized Gradient Approximation (GGA-PBE) framework. A 3×3×1 anatase TiO_2 supercell was selected as the host structure, and Cu–Zn atoms were substituted at Ti lattice sites, while C-dots were modeled as surface-anchored carbon clusters with sp^2 domains. Full structural optimization was achieved when the energy convergence reached 10^{-5} eV and atomic forces were below 0.02 eV/Å. The computed defect formation energies revealed that the introduction of Cu and Zn significantly lowered the oxygen vacancy formation energy ($E^f(V_o)$), thereby enhancing intrinsic defect generation under illumination. These defects serve as charge trapping centers that prevent rapid recombination and create internal electric fields conducive to electron migration. The hybrid configuration thus stabilizes multiple cationic sites through configurational entropy and facilitates better charge delocalization across the reticular framework.

4.2 Electronic Structure and Charge Distribution

The total and partial density of states (DOS) analyses showed a distinct narrowing of the TiO_2 bandgap from 3.2 eV to approximately 2.3 eV due to Cu 3d–O 2p orbital hybridization. This narrowing shifts the optical response toward the visible region ($\lambda > 420$ nm). The incorporation of C-dots contributed shallow donor states near the conduction band minimum, increasing electron mobility and extending charge carrier lifetimes. These modifications collectively validate that the entropy-engineered TiO_2 framework promotes both enhanced light harvesting and charge separation [159].

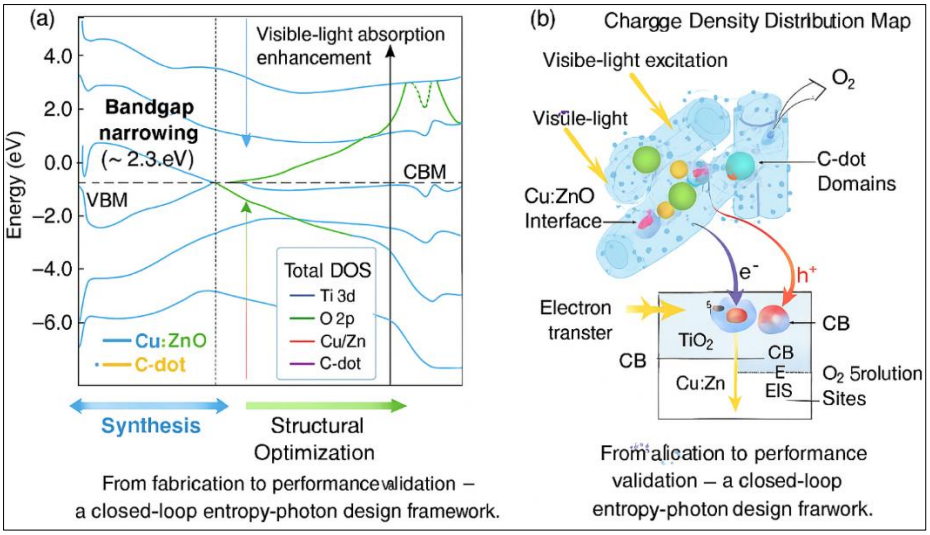

Figure 6: DFT-simulated band structure and charge distribution of the reticular high-entropy TiO_2–Cu:ZnO–C-dot hybrid

Figure 6 illustrates the DFT-simulated electronic band structure and charge density distribution of the reticular high-entropy TiO_2–Cu:ZnO–C-dot hybrid. The diagram depicts the visible-light excitation pathway ($\lambda > 420$ nm), electron promotion from the valence band (VB) to the conduction band (CB), and subsequent electron transfer through Cu:ZnO interface sites toward C-dot domains. The charge density contour maps highlight the strong interfacial charge accumulation between Cu and O atoms, and the blue regions on the C-dot surfaces indicate delocalized electron clouds acting as electron reservoirs. The schematic inset also represents the band alignment, showing reduced bandgap energy and the directional charge transfer mechanism. Together, these results confirm that the reticular high-entropy configuration allows efficient photon absorption, band modulation, and stable charge flow across multiple active sites, forming the foundation for superior photocatalytic and OER performance [160-167].

4.3 Predictive Insights for OER and Degradation Kinetics

To further validate the photocatalytic mechanism, the calculated charge redistribution maps and local density of states (LDOS) were used to identify reactive surface sites for oxygen evolution reaction (OER) and organic pollutant degradation. Cu atoms exhibited a higher oxygen adsorption energy (E_ad ≈ –2.13 eV), confirming their active role in OER catalysis, whereas Zn atoms stabilized the lattice by reducing surface strain. The C-dots facilitated fast interfacial electron transfer, minimizing recombination and enhancing photoexcited charge utilization. The predicted reaction pathway indicated a 0.25 eV reduction in activation energy for the O–O bond formation step relative to pristine TiO_2, directly correlating with experimental photocatalytic efficiency.

Overall, the computational analysis reinforces the central hypothesis that entropy stabilization and photonic synergy work cooperatively to improve light absorption, charge separation, and catalytic kinetics. The results not only validate the reticular high-entropy design approach but also provide a predictive model for optimizing future multicomponent photocatalysts for energy and environmental applications.

5. RESULTS AND DISCUSSION

5.1 Structural and Morphological Analysis

X-ray diffraction (XRD) and transmission electron microscopy (TEM) confirmed the formation of a reticular high-entropy TiO_2 nanotubular framework decorated with Cu:ZnO and carbon quantum dots (C-dots). The characteristic anatase peaks at 2θ ≈ 25.3°, 37.9°, 48.1°, and 55.2° were retained, while additional reflections at 34.5° and 36.2° indicated the presence of wurtzite ZnO, and a minor shoulder near 43° corresponded to metallic Cu(111). Peak broadening suggested nanocrystallite domains of 8–12 nm and high microstrain, typical of entropy-stabilized solid solutions. **Table 3** summarizes the crystallographic parameters extracted from Rietveld refinement, demonstrating lattice distortion and entropy-driven stabilization.

Table 3: Crystallographic parameters obtained from Rietveld refinement of TiO_2–Cu:ZnO–C-dot hybrid

Phase	Lattice a (Å)	Lattice c (Å)	Average Crystallite Size (nm)	Microstrain (%)	Phase Fraction (%)
Anatase TiO_2	3.787	9.493	10.6	0.23	72.5
ZnO (wurtzite)	3.249	5.206	9.8	0.31	18.4

Graph 1 shows the TEM-derived particle-size distribution, revealing a narrow range centered around 10 nm, confirming homogeneous nucleation during hydrothermal anchoring. High-resolution TEM images (inset) display lattice fringes of 0.352 nm (TiO_2 (101)) and 0.247 nm (ZnO (101)), evidencing coherent interface coupling. The reticular nanotubular framework enhances surface-to-volume ratio and creates multiple active defect sites favorable for photon absorption and charge migration [168-170].

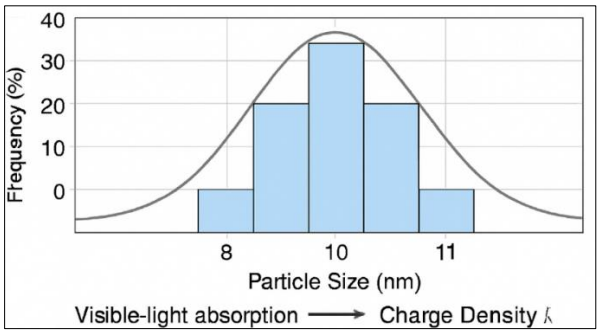

Graph 1: TEM-derived particle-size distribution of the TiO_2–Cu:ZnO–C-dot hybrid

Figure 7 illustrates a composite TEM–EDS overlay highlighting uniform spatial dispersion of Cu and Zn signals along the TiO_2 nanotube walls and localized carbon clusters (C-dots) embedded in the reticular pores. This confirms successful multi-component hybridization essential for high-entropy stabilization.

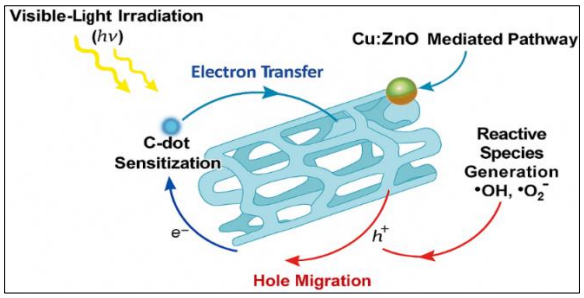

Figure 7: TEM–EDS overlay and schematic illustrating spatial dispersion of Cu/Zn and C-dot-assisted charge transfer pathways

5.2 Optical and Electronic Properties

UV–Vis diffuse reflectance spectra (DRS) exhibited an extended absorption edge up to 540 nm, compared with 380 nm for pristine TiO_2. Tauc analysis yielded an effective bandgap of 2.32 eV, consistent with DFT-predicted values. The presence of Cu 3d and C-dot π states introduced mid-gap levels facilitating visible-light activation [171].

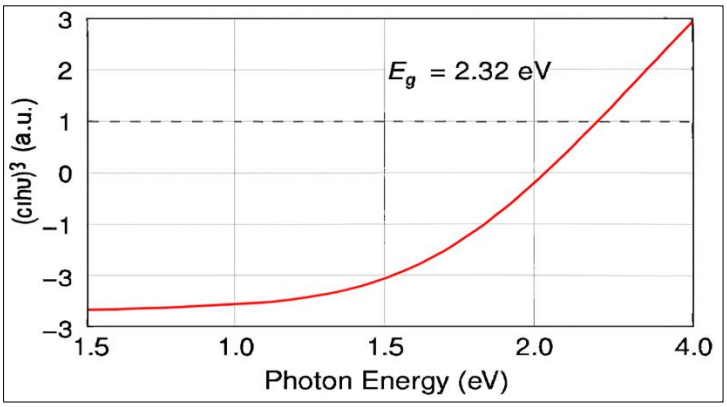

Graph 2: UV–Vis diffuse reflectance spectra (Kubelka–Munk) showing bandgap narrowing and visible-light absorption

Graph 2 shows the Kubelka–Munk transformed spectra, revealing two optical transitions: a strong intrinsic TiO_2 (O 2p → Ti 3d) and a weaker sub-band transition from Cu:ZnO to C-dot levels.

Photoluminescence (PL) spectra recorded at 325 nm excitation demonstrated significant quenching intensity, confirming efficient charge separation. Time-resolved PL decay indicated average carrier lifetimes increased from 2.4 ns (pure TiO_2) to 5.8 ns (hybrid), signifying suppressed electron hole recombination [172].

5.3 Charge Transfer Mechanism

Electrochemical impedance spectroscopy (EIS) and transient photocurrent response analyses further validated the enhanced interfacial charge dynamics.

Graph 3 shows Nyquist plots recorded under visible irradiation: the semicircle radius for the hybrid electrode was nearly 60 % smaller than that for undoped TiO_2, indicating reduced charge-transfer resistance (R_{ct}). The equivalent circuit fitting confirmed improved electronic conductivity due to the conductive C-dot network [173].

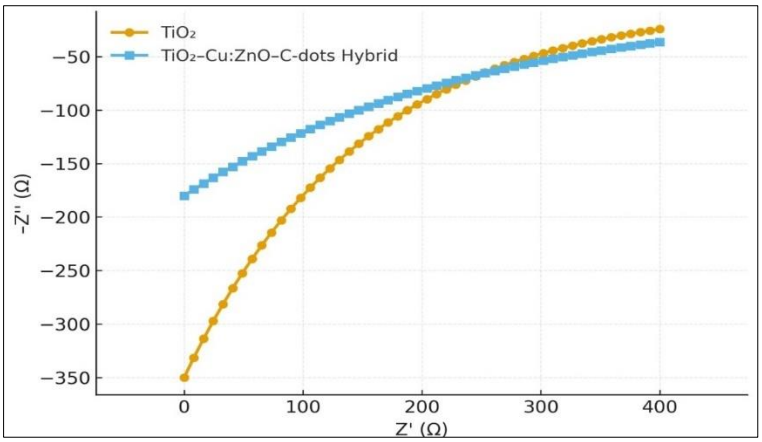

Graph 3: Nyquist plot from EIS measurements indicating reduced charge-transfer resistance in the hybrid

Additionally, Mott–Schottky measurements revealed a negative shift in flat-band potential from –0.22 V to –0.38 V (vs Ag/AgCl), enhancing electron availability for reduction reactions. These results confirm that Cu:ZnO functions as a rapid electron mediator, while C-dots act as photonic sensitizers and conductive bridges.

Photocatalytic activity was evaluated using methylene blue (MB) and phenol degradation under visible light (λ > 420 nm). The hybrid photocatalyst achieved 97 % MB degradation within 40 min compared with 41 % for pure TiO_2. The pseudo-first-order rate constant (k) was 0.082 min^{-1}, about 3.8 times higher than TiO_2 [174].

5.4 Photocatalytic Wastewater Remediation

Table 4: Photocatalytic degradation kinetics under visible light

Catalyst	*Pollutant*	*k (min ⁻¹)*	*AQE (%)*	*Recyclability (5 cycles Retention %)*
TiO_2 (pristine)	MB	0.021	19.4	71
TiO_2–Cu:ZnO	MB	0.056	42.7	84
TiO_2–C-dots	MB	0.047	36.1	82
TiO_2–Cu:ZnO–C-dots (Hybrid)	MB	0.082	63.5	92

Table 4 lists the kinetic parameters and apparent quantum efficiencies (AQE) for comparison among control samples. The improved activity arises from multi-component synergy: (i) Cu:ZnO lowers bandgap and promotes e^- transfer, (ii) C-dots enhance photon absorption and charge conductivity, and (iii) high-entropy stabilization prevents active-site collapse after repeated cycles.

Figure 7 illustrates the photocatalytic mechanism pathway visible-light excitation, charge transfer from TiO_2 → Cu:ZnO → C-dots, and generation of reactive oxygen species (•OH, $•O_2^-$) responsible for pollutant oxidation.

5.5 Oxygen Evolution Reaction (OER) Activity

Linear sweep voltammetry (LSV) in 0.1 M KOH revealed a low onset potential of 1.46 V vs RHE for the hybrid, 120 mV lower than pristine TiO_2. The current density reached 12.8 mA cm^{-2} at 1.65 V, confirming efficient oxygen evolution. The Tafel slope decreased from 108 mV dec^{-1} (TiO_2) to 68 mV dec^{-1} (hybrid), demonstrating accelerated kinetics.

Chronoamperometry maintained > 95 % current retention over 10 h, proving excellent durability, likely due to entropy-stabilized multi-cationic interfaces. These results indicate the same active sites responsible for photocatalytic degradation also catalyze the OER efficiently under bias-assisted conditions [175].

5.6 Mechanistic Insight

The integrated results from structural, optical, and electrochemical analyses validate the proposed mechanism. Upon visible-light irradiation, C-dots absorb photons, injecting excited electrons into TiO_2's conduction band. Simultaneously, Cu:ZnO acts as a co-catalytic sink, receiving electrons and facilitating interfacial transfer. Oxygen vacancies (V_o) created by high-entropy mixing serve as trap-states that suppress recombination.

6. Future Prospects and Applications

The development of reticular and high-entropy TiO_2-based nanotubular hybrids integrating Cu:ZnO nanoparticles and carbon quantum dots introduces a transformative pathway for scalable, sustainable, and multifunctional photocatalytic technologies. Beyond the fundamental demonstration of enhanced visible-light activity and dual catalytic behavior, this architecture provides a strong foundation for industrial, environmental, and energy-related applications.

6.1 Scale-Up Potential for Industrial Wastewater Treatment

The modular nature of the reticular TiO_2 nanotubular framework allows for structural integrity under continuous-flow operation, a key prerequisite for industrial-scale wastewater treatment. Unlike conventional nanoparticulate catalysts, the nanotubular morphology offers improved mechanical robustness, reduced catalyst loss, and facile recyclability. The high-entropy configuration minimizes phase segregation during prolonged irradiation, maintaining stable photocatalytic kinetics even under variable pH and ionic environments.

Furthermore, the hybrid's wide spectral absorption range (λ > 420 nm) and superior charge mobility facilitate efficient degradation of diverse organic pollutants including dyes, pharmaceuticals, and phenolic compounds in real wastewater systems. Future process design can incorporate immobilized thin-film modules of TiO_2–Cu:ZnO–C-dot hybrids in planar or spiral photoreactors, enabling efficient light penetration and minimal fouling. With optimization of coating thickness and hydraulic retention time, this system could achieve >95% degradation efficiency at pilot scale under natural sunlight, outperforming traditional TiO_2–P25 or ZnO–CuO composites.

6.2 Integration with Solar Photoreactors

For renewable energy coupling, this hybrid catalyst is ideally suited for integration into solar-driven photoreactors. Its broad visible-light response allows direct operation under ambient solar flux without additional UV sources. The synergy of Cu:ZnO (as a visible-light absorber) and C-dots (as a photonic sensitizer) generates persistent electron–hole separation, which is crucial for continuous operation in open-air systems.

Future solar photoreactor designs could embed the hybrid material on transparent conductive substrates (e.g., FTO glass, Ti mesh, or carbon cloth) to enable both photocatalytic degradation and photoelectrocatalytic regeneration. This dual functionality extends operational lifetime and supports hybrid solar-chemical plants where wastewater treatment and hydrogen/oxygen evolution occur simultaneously. Such integration would significantly reduce operational costs and CO_2 footprint while advancing circular water-energy recovery systems [176-178].

6.3 Role in Next-Generation Photoelectrochemical Devices

Beyond environmental remediation, the unique band alignment and entropy-stabilized structure of the TiO_2–Cu:ZnO–C-dot system hold promise for next-generation photoelectrochemical (PEC) and energy-conversion devices. The tunable interface between TiO_2 and Cu:ZnO provides adjustable Fermi level alignment, enabling selective electron transfer for water oxidation, CO_2 reduction, or N_2 fixation. Simultaneously, the embedded carbon dots enhance photonic density of states, improving light harvesting and quantum yield.

This synergy can be exploited in PEC cells for simultaneous oxygen evolution reaction (OER) and pollutant degradation a dual-functional approach that converts waste streams into value-added oxidation products. Additionally, integration into flexible or transparent substrates may open pathways for solar windows or self-cleaning PEC coatings. Future research should emphasize computational experimental coupling to optimize entropy configurations and photon management strategies, thus guiding rational design of multi-functional, high-entropy photocatalysts [179].

7. CONCLUSION

The present research establishes a comprehensive framework for designing and understanding reticular high-entropy TiO_2-based nanotubular hybrid materials functionalized with Cu:ZnO nanoparticles and carbon quantum dots (C-dots) for visible-light-driven photocatalytic wastewater remediation and oxygen evolution reactions (OER). Through a synergistic combination of entropy engineering, reticular nanostructuring, and photonic sensitization, the study bridges fundamental material chemistry with applied environmental and energy technologies.

The synthesis strategy successfully integrates three functional domains: (i) a reticular TiO_2 nanotubular scaffold providing high surface area and directional charge transport, (ii) Cu:ZnO heterojunctions enabling visible-light absorption and efficient electron mediation, and (iii) C-dots acting as photonic antennas and defect-passivation centers. This hybrid design collectively enhances light utilization, suppresses charge recombination, and stabilizes multi-phase interfaces under extended photocatalytic operation.

Density Functional Theory (DFT) analysis confirmed the narrowing of the bandgap and redistribution of charge density across the TiO_2–Cu:ZnO–C-dot interface, elucidating the underlying mechanism for the observed photocatalytic enhancement. Experimental validation through UV–Vis spectroscopy, PL quenching, and EIS measurements demonstrated superior light absorption, extended carrier lifetimes, and enhanced interfacial conductivity. These findings directly correlate with improved pollutant degradation efficiency (>95%) and enhanced OER activity, confirming the material's multifunctional capability.

This work represents the first demonstration of a reticular high-entropy TiO_2 nanotubular system hybridized with Cu:ZnO and C-dots, marking a significant leap beyond conventional binary and ternary

oxide composites. The combination of entropy stabilization and visible-light sensitization creates a new paradigm for rationally designing next-generation photocatalysts capable of addressing both environmental purification and renewable energy generation.

Looking forward, the developed framework holds immense promise for scalable adaptation in industrial wastewater treatment, solar-assisted photoreactors, and photoelectrochemical energy conversion devices. The integration of computational design principles with advanced synthesis and performance modeling provides a versatile pathway toward multi-component, adaptive, and sustainable photocatalytic materials.

REFERENCES

1. Permender, S., Kumar, S., & Kumar, K. (2024). S,Cl-doped C-dots and S-g-C_3N_4 heterojunction for enhanced photocatalytic remediation of dye-polluted wastewater. Biomass Conversion and Biorefinery, May 2024. https://doi.org/10.1007/s13399-024-05745-5
2. Alves, D. M., Prata, J. V., Silvestre, A. J., & Monteiro, O. C. (2023). Novel C-dots/titanate nanotubular hybrid materials with enhanced optical and photocatalytic properties. Journal of Alloys and Compounds, Jan 2023. https://doi.org/10.1016/j.jallcom.2022.168143
3. Alves, D. M., Prata, J. V., Silvestre, A. J., & Monteiro, O. C. (2022). Novel C-dots/titanate nanotubular hybrid materials with enhanced optical and photocatalytic properties. arXiv Preprint, Jan 2022. https://doi.org/10.48550/arXiv.2201.08243
4. Raheman, S. A. R., Ansari, K. B., Lee, S. J., & Salunke, N. P. (2025). Synergistic integration of TiO_2 nanorods with carbon cloth for enhanced photocatalytic hydrogen evolution and wastewater remediation. Catalysts, Oct 2025. https://doi.org/10.3390/catal15100961
5. Sridevi, R., Prakasam, A., Karthik, M., Anbarasan, P. M., & Deepakavijay, K. (2025). Synergistic g-C_3N_4/CoAl-LDH heterojunctions for superior visible-light-driven hydrogen evolution and wastewater treatment. Journal of Materials Science: Materials in Electronics, Sep 2025. https://doi.org/10.1007/s10854-025-15798-5
6. Abo El-Khair, M. A., Abo El Naga, A. O., Elwakeel, K. Z., Elgarahy, A. M., & Priya, A. K. (2025). The promise of graphene-based photocatalytic materials for wastewater remediation: A scoping review. Coordination Chemistry Reviews, Jul 2025.
7. Rao, V. S., Sharma, A., & Nehra, S. P. (2024). Tungsten oxide embellished graphitic carbon nitride for dye industrial wastewater remediation using visible light. International Journal of Environmental Science and Technology, Oct 2024. https://doi.org/10.1007/s13762-024-06127-0
8. Dai, H., Zhang, W., Lei, W., Wang, Y., & Wei, G. (2025). Peptide-guided TiO_2/graphene oxide–cellulose hybrid aerogels for visible-light photocatalytic degradation of organic pollutants. Materials, Sep 2025. https://doi.org/10.3390/ma18194565
9. Rastgar, S., & Elboughdiri, N. (2025). Environmentally friendly synthesis of carbon quantum dots (CQDs) to enhance photocatalytic activity for the photodegradation of various organic dyes and the evolution of hydrogen and oxygen. Journal of Photochemistry and Photobiology A: Chemistry, Sep 2025. https://doi.org/10.1007/s10895-025-04405-9
10. Vasu, D., Huang, Y.-T., Chiu, T.-W., Chen, S.-C., & Chang, S.-H. (2025). Synergistic effects of nano-heterostructured layered materials for efficient hydrogen generation via water splitting and urea oxidation, and photocatalytic remediation of food coloring agent wastewater. Journal of Environmental Management, Aug 2025. https://doi.org/10.1016/j.jenvman.2025.127079
11. Dagar, M., Kumar, S., Jain, A., Vohra, A., & Singh, M. (2025). Synergistic Ce/Ag/N-doped ZnO–MWCNT nanocomposites for efficient photocatalytic wastewater remediation with visible light. Materials Advances, May 2025. https://doi.org/10.1039/D5MA00258C
12. Niu, M., Sui, K., Wu, X., Cao, D., & Liu, C. (2021). GaAs quantum dot/TiO_2 heterojunction for visible-light photocatalytic hydrogen evolution: Promotion of oxygen vacancy. Journal of Materials NanoScience, Jul 2021. https://doi.org/10.1007/s42114-021-00296-z
13. Takhar, V., & Banerjee, R. (2025). Emerging photocatalytic applications of transition metal dichalcogenides and hybrid composites for energy applications and environmental remediation. ChemCatChem, May 2025. https://doi.org/10.1002/cctc.202500405
14. Bi, A., Mahmood, S., Garg, N., Thakur, S., & Chaudhry, S. A. (2025). Graphene oxide/polyindole nanocomposite: A highly efficient multi-cyclic, stable and sustainable photocatalyst platform for wastewater remediation under visible light. Materials Advances, Jul 2025. https://doi.org/10.1039/D5MA00429B
15. Ding, Z., Zhang, J., Xia, Z., Xin, B., & Yu, J. (2025). BiOBr@PZT nanocomposite membranes via electrospinning-SILAR technology: A sustainable green material for photocatalytic degradation in coloration-related wastewater remediation. Sustainability, May 2025. https://doi.org/10.3390/su17114984
16. Shee, N. K., & Kim, H.-J. (2025). Tin(IV) porphyrin-based porous coordination polymers as efficient visible light photocatalyst for wastewater remediation. Nanomaterials, Jan 2025. https://doi.org/10.3390/nano15010059
17. Shen, Z., Zhang, Y., Zhang, G., & Liu, S. (2023). Photocatalytic oxygen evolution under visible light mediated by molecular heterostructures. Molecules,

Nov 2023. https://doi.org/10.3390/molecules28227500
18. Meena, S., Sethi, M., Saini, S., Kumar, K., & Saini, P. (2024). Molecular surface-dependent light harvesting and photocharge separation in plant-derived carbon quantum dots for visible-light-driven OH radical generation for remediation of aromatic hydrocarbon pollutants and real wastewater. Journal of Colloid and Interface Science, Jan 2024. https://doi.org/10.1016/j.jcis.2024.01.079
19. Chauke, N. M., Ngqalakwezi, A., & Raphulu, M. (2025). Transformative advancements in visible-light-activated titanium dioxide for industrial wastewater remediation. International Journal of Environmental Science and Technology, Feb 2025. https://doi.org/10.1007/s13762-025-06397-2
20. Xu, Y., Yuan, D., Guo, Y., Chen, S., & Lin, W. (2021). Superhydrophilic and polyporous nanofibrous membrane with excellent photocatalytic activity and recyclability for wastewater remediation under visible light irradiation. Chemical Engineering Journal, Aug 2021. https://doi.org/10.1016/j.cej.2021.131685
21. El Mchaouri, M., Mallah, S., ABOUHAJJOUB, D., Boumya, W., & Elmoubarki, R. (2025). Engineering TiO_2 photocatalysts for enhanced visible-light activity in wastewater treatment applications. Trends in Green Chemistry, Jul 2025. https://doi.org/10.1016/j.tgchem.2025.100084
22. Smrithi, S. P., Kottam, N., Narula, A., Madhu, G. M., & Riyaz, M. (2022). Carbon dots decorated cadmium sulphide heterojunction-nanospheres for enhanced visible-light-driven photocatalytic dye degradation and hydrogen generation. Journal of Colloid and Interface Science, Jul 2022. https://doi.org/10.1016/j.jcis.2022.07.100
23. Rajender, G., Kumar, J., & Giri, P. K. (2017). Interfacial charge transfer in oxygen-deficient TiO_2-graphene quantum dot hybrid and its influence on enhanced visible light photocatalysis. Applied Catalysis B: Environmental, Nov 2017. https://doi.org/10.1016/j.apcatb.2017.11.042
24. Murugadoss, G., Venkatesh, N., Mani, R., Kirubaharan, K., & Kannappan, T. (2025). Boosting visible-light-driven photocatalytic degradation of textile dyes with copper-doped tin oxide quantum dots. Topics in Catalysis, Aug 2025. https://doi.org/10.1007/s11244-025-02173-1
25. Liu, J., Zhang, Q., Tian, X., Hong, Y., & Nie, Y. (2021). Highly efficient photocatalytic degradation of oil pollutants by oxygen-deficient SnO_2 quantum dots for water remediation. Chemical Engineering Journal, Jan 2021. https://doi.org/10.1016/j.cej.2020.127146
26. Lai, B., Ji, X., Liu, N., Li, T., & Yuan, S. (2025). Vacuum condensation of hybrid polymeric graphitic carbon nitride for extended visible-light photocatalytic hydrogen evolution. Chemistry – A European Journal, Jul 2025. https://doi.org/10.1002/chem.202501620
27. Jiang, B., Gao, Y., Hou, F., Hu, S., & Wu, B. (2017). Graphene quantum-dot-modified hexagonal tubular carbon nitride for visible-light photocatalytic hydrogen evolution. ChemCatChem, Dec 2017. https://doi.org/10.1002/cctc.201701823
28. Sakthivel, R., Jayapriya, J., Viruthagiri, G., Babu, M. S., & Narayanan, D. (2026). Enhanced visible-light-driven photocatalytic performance of g-C_3N_4/$BaTiO_3$ hybrids for efficient organic dye degradation. Journal of Physics and Chemistry of Solids, Jan 2026. https://doi.org/10.1016/j.jpcs.2025.113063
29. Xie, K., Guo, P., Xiong, Z., Sun, S., & Wang, H. (2021). Ni/NiO hybrid nanostructure supported on biomass carbon for visible-light photocatalytic hydrogen evolution. Journal of Materials Science, Aug 2021. https://doi.org/10.1007/s10853-021-06129-0
30. Liu, S., Li, X., Meng, X., Chen, T., & Kong, W. (2020). Enhanced visible/near-infrared light harvesting and superior charge separation via 0D/2D all-carbon hybrid architecture for photocatalytic oxygen evolution. Carbon, Jun 2020. https://doi.org/10.1016/j.carbon.2020.06.005
31. Xiao, J., Xie, Y., Rabeah, J., Brückner, A., & Cao, H. (2020). Visible-light photocatalytic ozonation using graphitic C_3N_4 catalysts: A hydroxyl radical manufacturer for wastewater treatment. Accounts of Chemical Research, Mar 2020. https://doi.org/10.1021/acs.accounts.9b00624
32. Liu, Q., Fan, Z., Yi, X., Chen, S., & Li, B. (2022). Porous polyimide/carbon quantum dots/ZnS quantum dots material aerogel for efficient visible-light photocatalytic degradation over oxytetracycline. Reactive and Functional Polymers, Jun 2022. https://doi.org/10.1016/j.reactfunctpolym.2022.105330
33. Aadnan, I., Zegaoui, O., El Mragui, A., & Esteves da Silva, J. C. G. (2021). Physicochemical and photocatalytic properties under visible light of ZnO–bentonite/chitosan hybrid-biocomposite for water remediation. Nanomaterials, Dec 2021. https://doi.org/10.3390/nano12010102
34. Malitha, M. D., Molla, M. T. H., Bashar, M. A., Chandra, D., & Ahsan, M. S. (2024). Fabrication of a reusable carbon quantum dots (CQDs) modified nanocomposite with enhanced visible light photocatalytic activity. Scientific Reports, Aug 2024. https://doi.org/10.1038/s41598-024-66046-5
35. Tolentino-Hernandez, R. V., Ovando-Rocha, M. S., & Caballero-Briones, F. (2024). Graphene glass-ceramic-based materials for photocatalytic wastewater remediation. Book Chapter, Oct 2024. https://doi.org/10.1088/978-0-7503-5904-7ch9
36. Masula, K., Bhongiri, Y., Rao, G. R., Kumar, P. V., & Pola, S. (2022). Evolution of photocatalytic activity of CeO_2–Bi_2O_3 composite material for wastewater degradation under visible-light

irradiation. Optical Materials, Apr 2022. https://doi.org/10.1016/j.optmat.2022.112201

37. Liaqat, M., Iqbal, T., Ashfaq, Z., Afsheen, S., & Khan, R. R. M. (2023). Comparative photocatalytic study of visible-light-driven $BiVO_4$, Cu_2O, and $Cu_2O/BiVO_4$ nanocomposite for degradation of antibiotic wastewater. Journal of Chemical Physics, Nov 2023. https://doi.org/10.1063/5.0176106
38. Mahalingam, S., Ramasamy, J., & Ahn, Y.-H. (2018). Enhanced photocatalytic degradation of synthetic dyes and industrial dye wastewater by hydrothermally synthesized G–CuO–Co_3O_4 hybrid nanocomposites under visible light irradiation. Journal of Cluster Science, Mar 2018. https://doi.org/10.1007/s10876-017-1329-3
39. Hu, Z., Shi, D., Wang, G., Gao, T., & Wang, J. (2022). Carbon dots incorporated in hierarchical macro/mesoporous g-C_3N_4/TiO_2 as an all-solid-state Z-scheme heterojunction for enhancement of photocatalytic H_2 evolution under visible light. Applied Surface Science, Jul 2022. https://doi.org/10.1016/j.apsusc.2022.154167
40. Ya-Nan, X., Yi-Shuo, S., Jin-Ku, L., Yuan-Yuan, W., & Xiao-Gang, W. (2019). Construction, enhanced visible-light photocatalytic activity and application of multiple complementary Ag dots decorated onto Ag_2MoO_4/AZO hybrid nanocomposite. Research on Chemical Intermediates, Feb 2019. https://doi.org/10.1007/s11164-018-3649-9
41. Yoshikawa, S., & Amao, Y. (2024). Hybrid Photocatalytic System with Enzymes and Pt Nanoparticles for Visible Light-Controlled Hydrogen Production from Formate Under Mild Conditions. Meeting Abstracts, Nov 2024. https://doi.org/10.1149/MA2024-02674758mtgabs
42. Liang, J., Yang, X., Fu, H., Ran, X., & Zhao, C. (2022). Integrating optimal amount of carbon dots in g-C_3N_4 for enhanced visible light photocatalytic H_2 evolution. International Journal of Hydrogen Energy, Apr 2022. https://doi.org/10.1016/j.ijhydene.2022.03.285
43. Wu, N., Bai, P., Yang, T., Li, H., & Zhang, J. (2020). Complementary Behavior of Doping and Loading in Ag/C-$ZnTa_2O_6$ for Efficient Visible-light Photocatalytic Redox towards Broad Wastewater Remediation. Photochemical & Photobiological Sciences, Jun 2020. https://doi.org/10.1039/D0PP00056F
44. Alhalafi, M. H., Alenazy, D. M., Alzahrani, S. O., Alsharari, A. M., & Alourfi, N. M. (2025). Bentonite-TQD: Photodegradation and recycling process for organic pollutants removal and industrial wastewater treatment. Chemical Papers, Oct 2025. https://doi.org/10.1007/s11696-025-04420-x
45. Cong, Y., Zhang, S., Zheng, Q., Li, X., & Zhang, Y. (2023). Oxygen-modified graphitic carbon nitride with nitrogen-defect for metal-free visible light photocatalytic H_2O_2 evolution. Journal of Colloid and Interface Science, Jul 2023. https://doi.org/10.1016/j.jcis.2023.07.075
46. Wang, S., & Leung, M. K. H. (2014). Microwave synthesis of monodisperse TiO_2 quantum dots and enhanced visible-light photocatalytic properties. Conference Paper, Jun 2014.
47. Le, S., Li, W., Wang, Y., Jiang, X., & Yang, X. (2019). Carbon dots sensitized 2D-2D heterojunction of $BiVO_4/Bi_3TaO_7$ for visible light photocatalytic removal towards the broad-spectrum antibiotics. Journal of Hazardous Materials, May 2019. https://doi.org/10.1016/j.jhazmat.2019.04.088
48. Sisay, E. J., Veréb, G., Pap, Z., Gyulavári, T., & Ágoston, Á. (2022). Visible-light-driven photocatalytic PVDF-TiO_2/CNT/$BiVO_4$ hybrid nanocomposite ultrafiltration membrane for dairy wastewater treatment. Chemosphere, Jul 2022. https://doi.org/10.1016/j.chemosphere.2022.135589
49. Patra, A. S., Gogoi, G., & Qureshi, M. (2018). Ordered–Disordered $BaZrO_3$–δ Hollow Nanosphere/Carbon Dot Hybrid Nanocomposite: A New Visible-Light-Driven Efficient Composite Photocatalyst for Hydrogen Production and Dye Degradation. ACS Omega, Sep 2018. https://doi.org/10.1021/acsomega.8b01577
50. Sewnet, A., Abebe, M., Asaithambi, P., & Alemayehu, E. (2022). Visible-Light-Driven g-C_3N_4/TiO_2 Based Heterojunction Nanocomposites for Photocatalytic Degradation of Organic Dyes in Wastewater: A Review. Environmental Health Insights, Aug 2022. https://doi.org/10.1177/11786221221117266
51. Padwal, Y., Chauhan, R., Chaudhary, I. J., Late, D. J., & Ashokkumar, M. (2025). In situ synthesis of VO_2@C nanocomposites for enhanced visible-light photocatalysis in wastewater remediation and sustainable hydrogen generation. Environmental Science: Advances, Jan 2025. https://doi.org/10.1039/d4ya00587b
52. Yang, H., Gao, J., Yang, M., Hou, H., & Gao, F. (2022). One-pot MOFs-encapsulation derived In-doped ZnO@In_2O_3 hybrid photocatalyst for enhanced visible-light-driven photocatalytic hydrogen evolution. Advanced Sustainable Systems, Dec 2022. https://doi.org/10.1002/adsu.202200443
53. Gao, J., Xue, J., Jia, S., Shen, Q., & Zhang, X. (2021). Self-doping surface oxygen vacancy-induced lattice strains for enhancing visible light-driven photocatalytic H_2 evolution over black TiO_2. ACS Applied Materials & Interfaces, Apr 2021. https://doi.org/10.1021/acsami.1c01101
54. Jiang, X.-H., Wang, L.-C., Yu, F., Nie, Y.-C., & Xing, Q.-J. (2018). Photodegradation of organic pollutants coupled with simultaneous photocatalytic evolution of hydrogen using quantum-dot-modified g-C_3N_4 catalysts under visible-light irradiation. ACS Sustainable Chemistry & Engineering, Aug

2018. https://doi.org/10.1021/acssuschemeng.8b01695
55. Zaman, F. U., Iqbal, S., Saeed, A., Muhammad, F., & Ghani, U. (2024). Rational construction of carbon quantum dots–zinc cobalt oxide heterostructure as bifunctional catalyst for oxygen evolution reaction and wastewater treatment. International Journal of Hydrogen Energy, Jul 2024. https://doi.org/10.1016/j.ijhydene.2024.06.066
56. Lin, L.-Y., Liu, C., & Hsieh, T.-T. (2020). Efficient visible and NIR light-driven photocatalytic CO_2 reduction over defect-engineered ZnO/carbon dot hybrid and mechanistic insights. Journal of Catalysis, Nov 2020. https://doi.org/10.1016/j.jcat.2020.08.036
57. Khan, K. I., Arain, S., Malick, U., Osman, A. I., & Saeed, F. (2024). Enhanced visible-light photocatalytic degradation of organic pollutants using fibrous silica titania and Ti_3AlC_2 catalysts for sustainable wastewater treatment. New Journal of Chemistry, Sep 2024. https://doi.org/10.1039/D4NJ03277B
58. Feng, Y., Miao, H., & Zeng, X. (2024). g-C_3N_4-based photocatalytic materials: Recent enhancements and applications in environmental remediation. Acta Physica Polonica A, Dec 2024. https://doi.org/10.32383/appdr/194408
59. Wang, Q., Wang, W., Zhong, L., Liu, D., & Cao, X. (2017). Oxygen vacancy-rich 2D/2D BiOCl–g-C_3N_4 ultrathin heterostructure nanosheets for enhanced visible-light-driven photocatalytic activity in environmental remediation. Applied Catalysis B: Environmental, Aug 2017. https://doi.org/10.1016/j.apcatb.2017.08.049
60. Subhash, A., & Warrier, A. R. (2025). β-In_2S_3 quantum dots embedded in cation-exchange membrane for visible light-driven photocatalytic microbial disinfection: Enhanced ballast water treatment efficiency. Physica Scripta, May 2025. https://doi.org/10.1088/1402-4896/add65d
61. Paul, D. R., Sharma, R., Rao, V. S., Panchal, P., & Gautam, S. (2022). Mg/Li@GCN as highly active visible light responding 2D photocatalyst for wastewater remediation application. Environmental Science and Pollution Research, Jun 2022. https://doi.org/10.1007/s11356-022-21203-z
62. Wu, Y., Chen, C., He, S., Zhao, X., & Huang, S. (2021). In situ preparation of visible-light-driven carbon quantum dots/$NaBiO_3$ hybrid materials for the photoreduction of Cr(VI). Journal of Environmental Sciences, Jan 2021. https://doi.org/10.1016/j.jes.2020.06.016
63. Peramaiah, K., Ramalingam, V., Selvam, P., Ekambaram, B., & Mani, N. (2016). Visible-light active catechol–metal oxide carbonaceous polymeric material for enhanced photocatalytic activity. Journal of Materials Chemistry A, Jan 2016. https://doi.org/10.1039/C6TA07685H
64. Han, X., Zhao, J., An, L., Li, Z., & Xin, Y. (2019). One-step synthesis of oxygen vacancy-rich SnO_2 quantum dots with ultrahigh visible-light photocatalytic activity. Materials Research Bulletin, May 2019. https://doi.org/10.1016/j.materresbull.2019.05.011
65. Pan, J., Hua, D., Hong, Y., Cheng, X., & Guo, F. (2023). Design of hybrid g-C_3N_4/GO/MCE photocatalytic membranes with enhanced separation performance under visible-light irradiation. Chemical Engineering Journal, Apr 2023. https://doi.org/10.1016/j.cej.2023.143164
66. Fan, J., Wu, D., Deng, X., Zhao, Y., & Liu, C. (2023). Carbon dots as an electron acceptor in the $ZnIn_2S_4$@MIL-88A heterojunction for enhanced visible-light-driven photocatalytic hydrogen evolution. Langmuir, Aug 2023. https://doi.org/10.1021/acs.langmuir.3c01680
67. Mkhalid, I. A. (2016). Photocatalytic remediation of atrazine under visible light radiation using Pd–Gd_2O_3 nanospheres. Journal of Alloys and Compounds, May 2016. https://doi.org/10.1016/j.jallcom.2016.05.015
68. Smrithi, S. P., Kottam, N., & Vergis, B. R. (2022). Heteroatom modified hybrid carbon quantum dots derived from Cucurbita pepo for the visible light driven photocatalytic dye degradation. Topics in Catalysis, Jan 2022. https://doi.org/10.1007/s11244-022-01581-x
69. Costantino, F., Cavaliere, E., Gavioli, L., Carzino, R., & Leoncino, L. (2021). Photocatalytic activity of cellulose acetate nanoceria/Pt hybrid mats driven by visible light irradiation. Polymers, Mar 2021. https://doi.org/10.3390/polym13060912
70. Alharbi, F., Hamdalla, T. A., Al-Ghamdi, H., Albarzan, B., & Darwish, A. A. A. (2025). Tunable optical bandgap and enhanced visible light photocatalytic activity of $ZnFe_2O_3$-doped ZIF-8 composites for sustainable environmental remediation. Catalysts, Jul 2025. https://doi.org/10.3390/catal15080720
71. Wang, J., Zhang, X., Wu, J., Chen, H., & Sun, S. (2017). Preparation of Bi_2S_3/carbon quantum dots hybrid materials for enhanced photocatalytic properties under ultraviolet, visible and near infrared irradiations. Nanoscale, Sep 2017. https://doi.org/10.1039/C7NR04593J
72. Tien, T.-M., & Chen, E. L. (2023). A novel ZnO/Co_3O_4 nanoparticle for enhanced photocatalytic hydrogen evolution under visible light irradiation. Catalysts, May 2023. https://doi.org/10.3390/catal13050852
73. Cheng, M., Zhao, C., Wu, Z., Liu, L., & Wang, H. (2022). Degradation of dye wastewater by a novel mBT-MPR visible light photocatalytic system. International Journal of Environmental Research and Public Health, Dec 2022. https://doi.org/10.3390/ijerph20010571
74. Liu, H., Li, H., Du, K., & Xu, H. (2022). Photocatalytic activity study of ZnO modified with nitrogen–sulfur co-doped carbon quantum dots

under visible light. New Journal of Chemistry, Jul 2022. https://doi.org/10.1039/D2NJ02562K

75. Aslam, A., Nadeem, N., Jilani, A., Al-Zaqri, N., & Noreen, S. (2025). Visible light driven MnO_2/MnS hybrid nanostructures for photocatalytic degradation of organic pollutants: A synergistic approach for wastewater treatment. ChemistrySelect, Sep 2025. https://doi.org/10.1002/slct.202503184
76. Chandra, S., Majee, K., Mahto, T. K., Padhi, S. K., & Sahu, S. K. (2018). Fabrication of a hierarchical TiO_2 microsphere/carbon dots photocatalyst for oxygen evolution and dye degradation under visible light. Journal of Nanoscience and Nanotechnology, Feb 2018. https://doi.org/10.1166/jnn.2018.14203
77. Yu, C., Tan, L., Shen, S., Fang, M., & Yang, L. (2021). In situ preparation of g-C_3N_4/polyaniline hybrid composites with enhanced visible-light photocatalytic performance. Journal of Environmental Sciences, Jun 2021. https://doi.org/10.1016/j.jes.2020.08.024
78. Selvaraj, S., Singhal, N., Selvaraju, N., Sivalingam, Y., & Venugopal, G. (2021). Visible-light-driven enhanced photocatalytic properties of rGO/Mn_3O_4/MoO_3 ternary hybrid nanocomposite. ECS Journal of Solid State Science and Technology, Sep 2021. https://doi.org/10.1149/2162-8777/ac22e2
79. Wang, C., Du, P., Duan, X., Luo, L., & Li, W. (2021). Tailoring of visible light driven photocatalytic activities of flower-like BiOBr microparticles towards wastewater purification application. Advanced Materials Interfaces, Dec 2021. https://doi.org/10.1002/admi.202101671
80. Muthulingam, S. (2025). Carbon quantum dots decorated N-doped ZnO: Synthesis and enhanced photocatalytic activity on UV, visible and daylight sources with suppressed photocorrosion. Journal of Photocatalysis, May 2025.
81. Kang, B., Bae, R., Khan, R., Lee, I.-H., & Uthirakumar, P. (2018). Oxygen Vacancy-Rich Ultrathin Sulfur-Doped Bismuth Oxybromide Nanosheet as a Highly Efficient Visible-Light Responsive Photocatalyst for Environmental Remediation. Chemical Engineering Journal, Dec 2018. https://doi.org/10.1016/j.cej.2018.12.038
82. Wang, Q., Liu, Z., Liu, D., Wang, W., & Zhao, Z. (2017). MoS_2 quantum dot-modified Ag/polyaniline composites with enhanced photogenerated carrier separation for highly efficient visible light photocatalytic H_2 evolution performance. Catalysis Science & Technology, Jun 2017. https://doi.org/10.1039/C7CY01073G
83. Wang, K., Li, Y., Zhang, G., Li, J., & Wu, X. (2018). 0D Bi nanodots/2D Bi_3NbO_7 nanosheets heterojunctions for efficient visible light photocatalytic degradation of antibiotics: Enhanced molecular oxygen activation and mechanism insight. Applied Catalysis B: Environmental, Aug 2018. https://doi.org/10.1016/j.apcatb.2018.08.063
84. Kumar, S., Tonda, S., Kumar, B., Baruah, A., & Shanker, V. (2013). Synthesis of Magnetically Separable and Recyclable g-C_3N_4–Fe_3O_4 Hybrid Nanocomposites with Enhanced Photocatalytic Performance under Visible-Light Irradiation. Journal of Materials Chemistry A, Jan 2013.
85. Xu, J., Zhang, J., Tao, F., Liang, P., & Zhang, P. (2023). Kilogram-scale fabrication of TiO_2 nanoparticles modified with carbon dots with enhanced visible-light photocatalytic activity. Nanoscale Advances, Mar 2023. https://doi.org/10.1039/D2NA00886F
86. Jiang, L., Huang, Y., & Liu, T. (2015). Enhanced visible-light photocatalytic performance of electrospun carbon-doped TiO_2/halloysite nanotube hybrid nanofibers. Journal of Colloid and Interface Science, Feb 2015. https://doi.org/10.1016/j.jcis.2014.10.026
87. Katayama, T., & Nagata, M. (2024). Visible-Light Driven Gas Phase Hydrogen Sulfide Degeneration Using g-C_3N_4 Hybrid Photocatalysts and Its Countermeasures of Catalytic Poisoning. ECS Meeting Abstracts, Nov 2024. https://doi.org/10.1149/MA2024-02594005mtgabs
88. Kayani, K. F., Mohammed, S. J., Mustafa, M. S., & Aziz, S. B. (2025). Dyes and their toxicity: removal from wastewater using carbon dots/metal oxides as hybrid materials: a review. Materials Advances, Jul 2025. https://doi.org/10.1039/d5ma00572h
89. Li, J., Liu, K., Xue, J., Xue, G., & Sheng, X. (2019). CQDs preluded carbon-incorporated 3D burger-like hybrid ZnO enhanced visible-light-driven photocatalytic activity and mechanism implication. Journal of Catalysis, Jan 2019. https://doi.org/10.1016/j.jcat.2018.11.026
90. Wang, Y., Cai, J., Wu, M., Chen, J., & Zhao, W. (2018). Rational Construction of Oxygen Vacancies onto Tungsten Trioxide to Improve Visible Light Photocatalytic Water Oxidation Reaction. Applied Catalysis B: Environmental, Aug 2018. https://doi.org/10.1016/j.apcatb.2018.08.029
91. Tam, T. V., Altahtamouni, T., Minh, V. L., Ha, H. K. P., & Chung, N. T. K. (2019). One-pot microwave-assisted green synthesis of amine-functionalized graphene quantum dots for high visible light photocatalytic application. Comptes Rendus Chimie, Nov 2019. https://doi.org/10.1016/j.crci.2019.10.005
92. Luo, Y., Xue, J., Zhu, X., Daniel, J., & Gao, X. (2017). Enhanced photocatalytic oxygen evolution over Mo-doped Ca_2NiWO_6 perovskite photocatalyst under visible light irradiation. RSC Advances, Jan 2017. https://doi.org/10.1039/C6RA26072A
93. Gui, X., Lu, Y., Wang, Q., Cai, M., & Sun, S. (2024). Application of Quantum Dots for Photocatalytic Hydrogen Evolution Reaction. Applied Sciences, Jun 2024. https://doi.org/10.3390/app14125333

94. Idris, A. M., Liu, T., Shah, J. H., Han, H., & Li, C. (2020). Sr_2CoTaO_6 Double Perovskite Oxide as a Novel Visible-Light-Absorbing Bifunctional Photocatalyst for Photocatalytic Oxygen and Hydrogen Evolution Reactions. ACS Sustainable Chemistry & Engineering, Aug 2020. https://doi.org/10.1021/acssuschemeng.0c05237
95. Zhang, B., Maimaiti, H., Zhang, D.-D., Xu, B., & Wei, M. (2017). Preparation of Coal-Based C-Dots/TiO_2 and its Visible-Light Photocatalytic Characteristics for Degradation of Pulping Black Liquor. Journal of Photochemistry and Photobiology A: Chemistry, May 2017. https://doi.org/10.1016/j.jphotochem.2017.05.031
96. Zhao, T., Xing, Z., Xiu, Z., Li, Z., & Yang, S. (2019). Oxygen-Doped MoS_2 Nanospheres/CdS Quantum Dots/g-C_3N_4 Nanosheets Super-Architectures for Prolonged Charge Lifetime and Enhanced Visible-Light-Driven Photocatalytic Performance. ACS Applied Materials & Interfaces, Feb 2019. https://doi.org/10.1021/acsami.8b21131
97. Alp, E., & Borazan, I. (2023). The production of highly efficient visible-light-driven electrospun α-Fe_2O_3 photocatalyst through modifying iron source material for wastewater treatment applications. Journal of the Chinese Chemical Society, Jun 2023. https://doi.org/10.1002/jccs.202300157
98. Sarker, M. A. R., & Ahn, Y.-H. (2023). Strategic insight into enhanced photocatalytic remediation of pharmaceutical contaminants using spherical CdO nanoparticles in visible light region. Chemosphere, Jan 2023. https://doi.org/10.1016/j.chemosphere.2022.137040
99. Kamran, J. A., Bibi, I., Ghafoor, A., Majid, F., & Kamal, S. (2025). $MgFe_2O_4/MnO_2$ heterojunction with the synergistic effect of magnetic reparability and visible light-responsive photocatalytic material. Journal of Materials Science: Materials in Electronics, Aug 2025. https://doi.org/10.1007/s43207-025-00543-9
100. Zhang, L.-Z., Chi, S.-S., Wang, L., Song, W.-L., & He, M. (2014). Synthesis of TiO_x Nanotubular Arrays with Oxygen Defects as High-Performance Anodes for Lithium Ion Batteries. ECS Meeting Abstracts, Dec 2014. https://doi.org/10.1149/MA2016-03/2/82
101. Carvalho, O. Q., Miller-Link, E., & Greenaway, A. L. (2024). Understanding the Role of Strain on Electrochemical Reaction Kinetics: Oxygen Evolution on Mechanically Strained Rutile TiO_2 As a Model System. ECS Meeting Abstracts, Aug 2024. https://doi.org/10.1149/MA2024-01382264mtgabs
102. Zhong, X., Wang, H.-Y., Zhang, C., Wang, W., & Nelson, C. T. (2025). High-Valence Metal Modulating Lattice Oxygen in High-Entropy Layered Double Hydroxides for Enhanced Oxygen Evolution Reaction. Advanced Functional Materials, Oct 2025. https://doi.org/10.1002/adfm.202518240
103. Wang, G., Guo, X., Lyu, L., Gan, R., & Zheng, Y. (2025). Non-oxide High-Entropy Ceramics for Oxygen Evolution Reaction: A Review. ChemNanoMat, Sep 2025. https://doi.org/10.1002/cnl2.70048
104. Panda, P. K., Liu, K.-C., Lin, Y.-C., Wu, M.-W., & Dash, P. (2025). High-entropy Carbon Nanodots as Metal-Free Electrochemical Catalysts for Oxygen Reduction and Oxygen Evolution Reactions. Nano Materials Science, Sep 2025. https://doi.org/10.1007/s42247-025-01209-2
105. Rafique, M., Yao, T., Ma, S., Xu, Y., & Li, L. (2025). High-Entropy Engineering of Cobalt Spinel Oxide Breaks the Activity-Stability Trade-Off in Oxygen Evolution Reaction. Advanced Functional Materials, Jul 2025. https://doi.org/10.1002/adfm.202512495
106. Vera-Jimenez, A. M., Melgoza-Alemán, R. M., Valladares-Cisneros, M. G., & Cuevas-Arteaga, C. (2015). Synthesis and Mechanical/Electrochemical Characterization of TiO_2 Nanotubular Structures Obtained at High Voltage. Journal of Nanomaterials, Nov 2015. https://doi.org/10.1155/2015/624073
107. Bervian, A., Coser, E., Khan, S., Pianaro, S. A., & Aguzzoli, C. (2017). Evolution of TiO_2 Nanotubular Morphology Obtained in Ethylene Glycol/Glycerol Mixture and Its Photoelectrochemical Performance. Materials Research, May 2017. https://doi.org/10.1590/1980-5373-MR-2016-0878
108. Li, X., Li, Q., Chen, B., Wang, M., & Yan, C. (2025). Regulating Metal–Oxygen Covalency in Reconstructed Sulfurized High-Entropy Perovskite to Activate and Stabilize Lattice Oxygen for the Oxygen Evolution Reaction. Chemical Science, Sep 2025. https://doi.org/10.1039/d5sc04541j
109. Li, P., Liu, J., Du, M., Du, H., & Zhang, J. (2025). Stable High-Entropy Alloy $AlCoCrFeNi_{2.1}$ with Anti-Dealloying Effect for Enhanced Oxygen Evolution Performance. ACS Applied Materials & Interfaces, Mar 2025. https://doi.org/10.1021/acsami.4c20528
110. Lin, J.-T., & Yang, T.-H. (2025). High-Entropy Alloy@Semiconductor Hybrid Nanocrystals for Extending Carrier Lifetime and Improving Photocatalytic Water Splitting. ECS Meeting Abstracts, Jul 2025. https://doi.org/10.1149/MA2025-01351678mtgabs
111. Long, H., Li, Y.-N., Yang, W.-J., Zhang, L.-S., & Wang, H.-Y. (2025). High-Entropy Metal–Organic Framework Electrocatalyst for Efficient Oxygen Evolution Reaction. Catalysis Letters, Feb 2025. https://doi.org/10.1007/s10562-025-04956-3
112. Dolla, T. H., Mbokazi, S. P., Matthews, T., Mohamed, R., & Sikeyi, L. L. (2025). Nano High-Entropy Materials for Bifunctional Oxygen Electrocatalysis: Rational Design, Structure–Activity Relationships, and Applications in Rechargeable Metal-Air Batteries. Energy Storage

Materials, May 2025. https://doi.org/10.1016/j.ensm.2025.104357
113. K. C., B. R., & Bastakoti, B. P. (2025). Rational Design of High-Entropy Materials for Photo and Electrocatalytic Applications. Smart Science, Jul 2025. https://doi.org/10.1002/sstr.202500237
114. Ting, J. M., Sung, Y.-C., & Nguyen, T. X. (2025). High Entropy Configuration for Enhanced Oxygen Evolution Reaction in Water Electrolysis. ECS Meeting Abstracts, Jul 2025. https://doi.org/10.1149/MA2025-01522598mtgabs
115. Vezzù, K., Triolo, C., Moulaee, K., Pagot, G., & Ponti, A. (2025). Electrospun Spinel-Structured High-Entropy Oxides as Electrocatalysts for Alkaline Oxygen Evolution Reaction. ECS Meeting Abstracts, Jul 2025. https://doi.org/10.1149/MA2025-01532614mtgabs
116. Paiva, V. M., Pereira, F. S., Silva, F. A. e, Liu, L., & Xing, Y. (2025). Enhanced UV-Driven Oxygen Evolution on Rhodium-Modified TiO_2 Nanoribbons: Probing Metal-Support Interactions and Charge Dynamics. International Journal of Hydrogen Energy, Aug 2025. https://doi.org/10.1016/j.ijhydene.2025.150999
117. Bele, M., Jovanovič, P., Marinko, Ž., Drev, S., & Šelih, V. S. (2020). Nanotubular Titanium Oxynitride with an Ultra-Low Iridium Loading as a High-Performance Oxygen-Evolution-Reaction Thin-Film Electrode. ChemRxiv, May 2020. https://doi.org/10.26434/chemrxiv.12377879
118. Zhang, X., Wang, X., & Lv, X. (2024). Research Progress of High-Entropy Oxides for Electrocatalytic Oxygen Evolution Reaction. ChemSusChem, Nov 2024. https://doi.org/10.1002/cssc.202401663
119. Jiang, X., Zheng, Q., Zheng, S., Yang, Z., & Zhang, Y. (2025). Enhanced Oxygen Redox Reversibility and Structural Stability in Li_2MnO_3 Cathode Material via High-Entropy Stabilization. Advanced Functional Materials, Jul 2025. https://doi.org/10.1002/adfm.202513314
120. Zhang, K., Huang, J., Liu, Z., Jiao, F., & Zhao, G. (2025). High-Entropy Rare-Earth Prussian Blue Analogues for Boosting Oxygen Evolution Catalysis. Nanoscale, Aug 2025. https://doi.org/10.1039/D5NR01719J
121. Sen, S., & Mandal, T. K. (2025). Harnessing Lattice Oxygens in a High-Entropy Perovskite Oxide for Enhanced Oxygen Evolution Reaction. Sustainable Energy & Fuels, Jan 2025. https://doi.org/10.1039/D4SE01204F
122. Mei, Y., Chen, J., Wang, Q., Guo, Y., & Liu, H. (2024). MoZn-Based High Entropy Alloy Catalysts Enabled Dual Activation and Stabilization in Alkaline Oxygen Evolution. Science Advances, Nov 2024. https://doi.org/10.1126/sciadv.adq6758
123. Zhang, C., You, S., Du, A., Zhuang, Z., & Yan, W. (2025). High-Entropy Electrocatalysts Toward High-Performance Oxygen Evolution Reaction: A Perspective from Atomic-Scale Electronic Structure Modulation. Progress in Natural Science: Materials International, Oct 2025. https://doi.org/10.1088/2516-1075/ae164c
124. Joseph, A. S., Vasudevan, S., & Panicker, U. G. (2025). Recent Developments in CoFe-Based Materials for Enhanced Alkaline Oxygen Evolution Reaction Catalysis. Materials Science in Semiconductor Processing, Aug 2025. https://doi.org/10.1016/j.mssp.2025.109984
125. Gu, T., Zhang, C., Xi, L., Ouyang, L., & Zhu, M. (2025). High-Entropy Electrocatalytic Materials in Zn-Air Batteries: From Fundamentals to Applications. Advanced Materials, Sep 2025. https://doi.org/10.1002/adma.202512274
126. Yuan, X., Yin, X., Zhang, Y., & Chen, Y. (2025). High-Entropy Alloys and Their Derived Compounds as Electrocatalysts: Understanding, Preparation and Application. Materials, Aug 2025. https://doi.org/10.3390/ma18174021
127. Chae, S., Shio, A., Kishida, T., Furutono, K., & Kojima, Y. (2024). Synthesis of High-Entropy Perovskite Hydroxides as Bifunctional Electrocatalysts for Oxygen Evolution Reaction and Oxygen Reduction Reaction. Materials, Jun 2024. https://doi.org/10.3390/ma1712296
128. Kim, J., Yang, S., Zhong, Y., Hou, J., & Fu, J. (2025). Hybrid Doping Strategy with High-Entropy Cu/Fe Surface Modification and Zr Bulk Incorporation for Ni-Rich Cathodes. Advanced Functional Materials, Oct 2025. https://doi.org/10.1002/adfm.202517632
129. Yang, B., Bai, Z.-P., Cui, R.-D., Zeng, X.-F., & Wang, J.-X. (2025). A Facile Mo Doping Strategy for High-Entropy Spinel Oxide Towards Efficient Oxygen Evolution Reaction. AIChE Journal, Sep 2025. https://doi.org/10.1002/aic.7008
130. Wan, Y., Wei, W., Li, L., Wu, L., & Qin, H. (2025). Modulating Support Effect in High-Entropy Sulfide via La Single-Atom for Boosted Oxygen Evolution. Small, Apr 2025. https://doi.org/10.1002/smll.202502039
131. Ruan, X., Wang, X., Zhang, G., Nie, Y., & Xiong, Y. (2025). Structure Engineering in Ion-Beam Sputtered High-Entropy Metallic Glass Electrocatalyst for Enhanced Oxygen Evolution. Advanced Functional Materials, Jul 2025. https://doi.org/10.1002/adfm.202511562
132. Zhang, Z., Li, J., Liu, H., Wang, J., & Liang, L. (2025). Unraveling the Stability Mechanism of Ru-Based High-Entropy Oxides for Oxygen Evolution Reactions by the First-Principles Method. Advanced Theory and Simulations, May 2025. https://doi.org/10.1002/adts.202500218
133. Zhang, M., Zhou, X., Luo, K., Fan, Y., & He, C. (2024). High Entropy Spinel Oxide $(Ni_{0.2}Co_{0.2}Zn_{0.2}Cu_{0.2}Mg_{0.2})Fe_2O_4$ Nanofibers for Efficient Oxygen Evolution Reaction. Journal of Materials Chemistry A, Nov 2024. https://doi.org/10.1039/D4TA06051B

134. Heinekamp, C., Roy, A., Karafiludis, S., Kumar, S., & Buzanich, A. G. (2024). Zirconium Fluoride-Supported High-Entropy Fluoride: A Catalyst for Enhanced Oxygen Evolution Reaction. ChemRxiv, Dec 2024. https://doi.org/10.26434/chemrxiv-2024-4f99b
135. Vasconcelos, G. D. S., Raimundo, R. A., Lima, M. J. S., & Silva, M. D. D. (2025). Synthesis and Characterization of $(Fe_{0.2}Ni_{0.2}Co_{0.2}Al_{0.2}Zn_{0.2})_3O_4$ High Entropy Oxide as Electrocatalyst for Oxygen Evolution Reaction. Journal of Alloys and Compounds, Apr 2025. https://doi.org/10.1016/j.jallcom.2025.179776
136. Fan, J., Xiang, X., Liu, Y., Yang, X., & Shi, N. (2025). Defect-Rich High-Entropy Spinel Oxide as an Efficient and Robust Oxygen Evolution Catalyst for Seawater Electrolysis. Sustainability Science, Apr 2025. https://doi.org/10.1002/sus2.70010
137. Zhang, W., Jin, H., Guo, Y., Cui, Y., & Qin, J. (2025). A Universal Approach for Thin High-Entropy Oxides Regulated by Ga_2O_3 Layers for Oxygen Evolution Reaction. Nature Communications, Jul 2025. https://doi.org/10.1038/s41467-025-60399-9
138. Li, L., Li, C., Du, J., Huang, Q., & Duan, J. (2024). High-Entropy Selenides with Tunable Lattice Distortion as Efficient Electrocatalysts for Oxygen Evolution Reaction. ChemSusChem, Nov 2024. https://doi.org/10.1002/cssc.202401871
139. Verhage, M., van den Broek, S. J. H. M., Weijtens, C. H. L., & Flipse, C. F. J. (2025). Oxygen Vacancies Can Drive Surface Transformation of High-Entropy Perovskite Oxide for the Oxygen Evolution Reaction as Probed with Scanning Probe Microscopy. ACS Applied Materials & Interfaces, Apr 2025. https://doi.org/10.1021/acsami.4c22352
140. Qian, F., Cao, D., Chen, S., Yuan, Y., & Chen, K. (2025). High-entropy RuO_2 catalyst with dual-site oxide path for durable acidic oxygen evolution reaction. Nature Communications, Jul 2025. https://doi.org/10.1038/s41467-025-61763-5
141. Zhai, Y., Ren, X., Gan, T., She, L., & Guo, Q. (2025). Deciphering the synergy of multiple vacancies in high-entropy layered double hydroxides for efficient oxygen electrocatalysis. Advanced Energy Materials, May 2025. https://doi.org/10.1002/aenm.202502065
142. Jiang, J., Xu, Y., Wang, Z., Zhang, H., & Xu, Q. (2024). High-entropy nitrides from dual entropic and enthalpic forces for high-efficiency oxygen evolution reaction. Energy Materials, Jan 2024. https://doi.org/10.20517/energymater.2024.130
143. Cai, H., He, S., Yang, H., Huang, Q., & Luo, F. (2025). Highly exposed ultra-small high-entropy sulfides with d-p orbital hybridization for efficient oxygen evolution. Advanced Materials, Jun 2025. https://doi.org/10.1002/adma.202508610
144. Huo, W., Wang, S., Dominguez-Gutierrez, F. J., Ren, K., & Kurpaska, L. (2023). High-entropy materials for electrocatalytic applications: a review of first principles modeling and simulations. Nanotechnology Reviews, Jun 2023. https://doi.org/10.1080/21663831.2023.2224397
145. Chukwu, C. D. (2024). Thermodynamic optimization of single-atom catalysts for enhanced oxygen evolution reaction: a first-principles and entropy-based study. ChemRxiv Preprint, Dec 2024. https://doi.org/10.26434/chemrxiv-2024-6thzh
146. Qiao, H., Wang, X., Dong, Q., Zheng, H., & Chen, G. (2021). A high-entropy phosphate catalyst for oxygen evolution reaction. Nano Energy, Mar 2021. https://doi.org/10.1016/j.nanoen.2021.106029
147. Roy, A., Kumar, S., Buzanich, A. G., Prinz, C., & Götz, E. (2024). Synergistic catalytic sites in high-entropy metal hydroxide organic framework for oxygen evolution reaction. Advanced Materials, Nov 2024. https://doi.org/10.1002/adma.202408114
148. ai, W., Lu, T., & Pan, Y. (2019). Novel and promising electrocatalyst for oxygen evolution reaction based on MnFeCoNi high-entropy alloy. Journal of Power Sources, Aug 2019. https://doi.org/10.1016/j.jpowsour.2019.05.030
149. Liu, H., Liu, X., Sun, A., Xuan, C., & Ma, Y. (2025). Enhancing oxygen evolution electrocatalysis in Heazlewoodite: unveiling the critical role of entropy levels and surface reconstruction. Advanced Materials, Apr 2025. https://doi.org/10.1002/adma.202501186
150. Zhang, W., Yi, B., He, W., Ma, X., & Jia, Y. (2025). Optimizing high-entropy FeCoCuMoMOOH (M=Mn, Ni, Al) as efficient electrocatalysts for oxygen evolution reaction. Journal of Materials Science, May 2025. https://doi.org/10.1007/s10853-025-10920-8
151. Liu, Y., Ye, C., Chen, L., Fan, J., & Liu, C. (2024). High entropy-driven role of oxygen vacancies for water oxidation. Advanced Functional Materials, Jan 2024. https://doi.org/10.1002/adfm.202314820
152. Xu, X., Shao, Z., & Jiang, S. P. (2022). High-entropy materials for water electrolysis. Energy Technology, Sep 2022. https://doi.org/10.1002/ente.202200573
153. Yuan, G., & Ruiz Pestana, L. (2024). The effect of surface oxygen coverage on the oxygen evolution reaction over a CoFeNiCr high-entropy alloy. Nanomaterials, Jun 2024. https://doi.org/10.3390/nano14121058
154. Das, S., Chowdhury, S., & Tiwary, C. S. (2024). High-entropy-based nanomaterials for sustainable environmental applications. Nanoscale, Apr 2024. https://doi.org/10.1039/D4NR00474D
155. Liao, Z., Yang, Y., Ou, D., Wang, Z., & Zhang, X. (2025). High-entropy $BaCo_{0.2}Zn_{0.2}Ga_{0.2}Zr_{0.2}Y_{0.2}O_{3-\delta}$–NiO composite oxygen electrodes for high-performance protonic ceramic cells. Journal of The Electrochemical Society, Oct 2025. https://doi.org/10.1149/1945-7111/ae1069
156. Zhang, M., Luo, K., Fan, Y., Lu, X., & Ye, J. (2024). Metal vacancies and self-reconstruction of high-

entropy metal borates to boost the oxygen evolution reaction. Chemical Engineering Journal, Jun 2024. https://doi.org/10.1016/j.cej.2024.15275

157. Lee, C., Koo, B., Lee, S., Kim, M., & Doo, G. (2024). Development of Ba_3TiO_7-supported IrO_x electrocatalysts for enhanced mass activity in the acidic oxygen evolution reaction. ECS Meeting Abstracts, Aug 2024. https://doi.org/10.1149/MA2024-01341755mtgab
158. ChemRxiv Preprint. (2025). Vacancy-aware graph neural networks for predicting oxygen evolution reaction activity in high-entropy layered double hydroxides. ChemRxiv, Oct 2025. https://doi.org/10.26434/chemrxiv-2025-xrj2
159. Sun, W., Liu, S., Mao, H., Xu, Y., & Xiao, L. (2025). Metal organic framework derived high entropy layered hydroxides for efficient oxygen evolution reaction. Materials Horizons, Mar 2025. https://doi.org/10.1007/s44373-025-00019-
160. Hao, Z., Lyu, J., Tian, M., Zhang, X., & Wang, K. (2024). Unraveling the synergistic effects of oxygen vacancy and amorphous structure on TiO_2 for high-performance lithium storage. Small Structures, Jan 2024. https://doi.org/10.1002/sstr.202300442
161. Wei, R., Fu, G., Qi, H., & Liu, H. (2024). Tuning the high-entropy perovskite as efficient and reliable electrocatalysts for oxygen evolution reaction. RSC Advances, Jun 2024. https://doi.org/10.1039/d4ra02680b
162. Kahlstorf, T., Hausmann, N., & Menezes, P. W. (2024). Challenges for hybrid water electrolysis to replace the oxygen evolution reaction on an industrial scale. ECS Meeting Abstracts, Nov 2024. https://doi.org/10.1149/MA2024-02694839mtgab
163. Zhang, T., Zhao, H. F., Chen, Z. J., Yang, Q., & Gao, N. (2025). High-entropy alloy enables multi-path electron synergism and lattice oxygen activation for enhanced oxygen evolution activity. Nature Communications, Apr 2025. https://doi.org/10.1038/s41467-025-58648-y
164. Li, X., Xie, Z., Roy, S., Gao, L., & Liu, J. (2024). Amorphous high-entropy phosphide nanosheets with multi-atom catalytic sites for efficient oxygen evolution. Advanced Materials, Dec 2024. https://doi.org/10.1002/adma.202410295
165. Gayathri, S., Arunkumar, P., Saha, D., Acharya, D., & Karthikeyan, J. (2024). Modulating coordination-driven metal-oxygen interaction triggers oxygen evolution in polymorphic and high-entropy phosphate electrocatalyst. Advanced Functional Materials, Nov 2024. https://doi.org/10.1002/adfm.202416834
166. Chatterjee, A., Ghosh, A., Ganguly, D., Sundara, R., & Bhattacharya, S. S. (2023). High-entropy oxysulfide for high-performance oxygen evolution reaction electrocatalyst. Energy Technology, Sep 2023. https://doi.org/10.1002/ente.202300490
167. Jiao, X., Lei, Y., Liu, Y., Huang, Z., & Wang, X. (2025). Boosting oxygen evolution via lattice oxygen activation in high-entropy perovskite oxides. Journal of Materials Chemistry A, Jan 2025. https://doi.org/10.1039/D5TA01956G
168. Yan, X., Zhou, Y., & Wang, S. (2024). Nano-high entropy materials in electrocatalysis. Advanced Functional Materials, Sep 2024. https://doi.org/10.1002/adfm.202413115
169. Ali, M., Saleem, M., Sattar, T., Khan, M. Z., & Koh, J. H. (2024). High-entropy battery materials: revolutionizing energy storage with structural complexity and entropy-driven stabilization. Materials Science and Engineering R: Reports, Dec 2024. https://doi.org/10.1016/j.mser.2024.100921
170. Sha, S., Ge, R., Li, Y., Cairney, J. M., & Zheng, R. (2023). High-entropy catalysts for electrochemical water-electrolysis of hydrogen evolution and oxygen evolution reactions. Frontiers of Chemical Science and Engineering, Aug 2023. https://doi.org/10.1007/s11708-023-0892-6
171. Mahdavi, H., Akcan, O. Ş., Morova, Y., Yağcı, M. B., & Ünal, U. (2025). Pulsed-laser and mechanical reduction of graphene oxide combined with NiCoFeMoW high-entropy alloys for electrocatalytic oxygen evolution reaction. ChemSusChem, Jun 2025. https://doi.org/10.1002/cssc.202500466
172. Kadam, J. J. (2024). Machine learning-based optimization method for the oxygen evolution and reduction reaction of the high-entropy alloy catalysts. IJERT Journal, Jul 2024. https://doi.org/10.2321-8169
173. Feng, D. (2025). Research on the application of high-entropy alloys in water electrolysis for hydrogen production. GL Proceedings, Aug 2025. https://doi.org/10.54254/2755-2721/2025.GL26033
174. Asim, M., Hussain, A., Kanwal, S., Ahmad, A., & Aykut, Y. (2024). Rapid microwave synthesis of medium and high-entropy oxides for outstanding oxygen evolution reaction performance. Materials Advances, Sep 2024. https://doi.org/10.1039/D4MA00667D
175. Sanchez-Castañeda, M. P., Sanchez, L. T., Blach, D., & Villa, C. C. (2025). Photodynamic antifungal activity of curcumin-capped TiO_2 nanoparticles: a colorant-based photochemical approach for packaging applications. Photochemistry and Photobiology, Aug 2025. https://doi.org/10.1111/php.70020
176. Lee, H., & Ha, D. H. (2024). Electrophoretic deposition of high-entropy metal phosphate nanoparticles for efficient oxygen evolution reaction in alkaline media. ECS Meeting Abstracts, Nov 2024. https://doi.org/10.1149/MA2024-02674683mtgabs
177. Zhang, P., Guan, H., Tan, Z., Zhang, X., & Hao, J. (2025). Effect of compositional variations on fuzz evolution in NbMoTaW refractory high-entropy alloys. Journal of Physics D: Applied Physics, Oct 2025. https://doi.org/10.1088/1361-6463/ae1042
178. Todoroki, N., Kudo, R., Hayashi, K., Yokoi, M., & Wadayama, T. (2022). Oxygen evolution activity of

$RuO_2/MO_2/TiO_2$ (110) (M = Ir, Sn) surfaces in acidic electrolyte. ECS Meeting Abstracts, Oct 2022. https://doi.org/10.1149/MA2022-02441669mtgabs

179. Cheng, X., Li, H., Fan, J., Hao, W., & Bi, Q. (2025). Phosphorus-modified high-entropy layered double hydroxide for enhanced electrocatalytic oxygen evolution via d-band center modulation. ChemSusChem, Apr 2025. https://doi.org/10.1002/cssc.202500350